Quantum-limited phase-matching effect in a Λ-type laser system

Deshui Yu[1,*] and Jingbiao Chen[2,†]

[1]*Department of Applied Physics, The University of Tokyo, Bunkyo-ku, Tokyo 113-8656, Japan*

[2]*Institute of Quantum Electronics, and State Key Laboratory of Advanced Optical Communication System & Network, School of Electronics Engineering & Computer Science, Peking University, Beijing 100871, P.R. China*

(Received 9 March 2011; published 29 June 2011)

The theory of a quantum-limited phase-matching effect in a Λ-type lasing system is studied in detail based on the quantum Langevin approach. Two quasimonochromatic fields are directly generated based on two lasing transitions. We find that the coherence between two lasers can well exceed the linewidth of either laser field. This result denotes that two field phases match each other although either laser field has a high phase fluctuation. Unlike the phase-matching effect based on atomic absorption, the final coherence between two laser fields here is not limited by saturation broadening, and the higher laser intensities lead to a higher coherence. Additionally, based on a linear stability analysis, we find that the instability of the field steady state can substantially restrict the occurrence of this phase-matching effect in the bad-cavity limit for a high pump rate. We also discuss the spectrum of amplitude fluctuations of output fields, and the result shows that the squeezing of amplitude fluctuations at low frequencies for a single field oscillating inside the cavity is damaged in the case of two fields oscillating.

DOI: 10.1103/PhysRevA.83.063846 PACS number(s): 42.55.Ah, 42.60.Da, 42.50.Ar

I. INTRODUCTION

The quantum-limited linewidth of a single-mode laser with a homogeneously broadened two-level medium can be expressed as [1–3]

$$D_{\mathrm{ST}} = \left(\frac{\gamma_{ab}}{\gamma_{ab}+\kappa}\right)^2 \frac{g^2\mathcal{N}_{a0}}{\mathcal{I}_0\gamma_{ab}}, \tag{1}$$

where $\mathcal{N}_{a0}$ is the steady-state value of the upper lasing level, γ_{ab} is the damping rate of atomic polarization, κ is the loss rate of the cavity, g is the atom-cavity coupling constant, and $\mathcal{I}_0$ is the photon number inside the cavity. Here we have used the same symbols as in Ref. [1]. For a given system, the quantum-limited laser linewidth is determined by the efficiency of atoms on the upper lasing level to produce the coherent photons, $\mathcal{I}_0/\mathcal{N}_{a0}$. D_{ST} corresponds to the well-known Schawlow-Townes (ST) linewidth [4] and is suitable in both good- and bad-cavity limits. The quantum-limited linewidth of a bad-cavity laser has been experimentally researched in Ref. [5]. The influence of the finite atom-field interaction time on the laser linewidth has been investigated in Ref. [6].

How to exceed the quantum limit described by D_{ST} has played an important role in quantum optics. The fundamental noise source of a laser system arises from the addition of spontaneously emitted photons with random phases to the coherent field. This quantum noise can be suppressed below the standard Schawlow-Townes limit by preparing the atomic system in coherent superposition [7,8] of states as in the Hanle effect and quantum beat experiments. In Ref. [9], the authors discussed the theory of quenching quantum fluctuations of a laser system with a ladder-type configuration. By using an external field to link the lower lasing level with another atomic level, whose decay rate is much larger, laser intensity significantly increases and the quantum-limited linewidth can be quenched. Cooperative interaction also has been introduced to the lasing process to reduce the quantum noise [10–13]. As a result, the field intensity can be enhanced by N times that of the usual lasers, while the linewidth is found to be extremely small, $D_{\mathrm{ST}} \sim 1/N^2$, where N is the number of atoms contributing to the laser field.

In Refs. [14,15], a scheme based on the phase-matching effect of the nonadiabatic interaction of two quasimonochromatic fields with Λ-type atoms has been investigated, and the corresponding experimental verification has been demonstrated in Ref. [16], in which the initial beam linewidth of 1 MHz between two lasers can be reduced to 5 kHz. In Ref. [17], the authors proposed to apply this phase-matching effect to the optical clock so as to get an optical frequency standard with an uncertainty of 1 mHz. However, this phase-matching effect is based on the stimulated absorption, and the final coherence between two laser fields is limited by the saturation broadening of two atomic transitions. It is difficult to get an extremely high coherence with high intensities of two laser fields. Actually, the phase-matching effect happens even in usual lasers (oscillating at single transition). The coherence between two longitudinal modes can be better than the stability of the individual modal phase. This is true not only for the mode-locked lasers [18], but also for multi-mode cw lasers.

In this article, we theoretically investigate the quantum-limited phase-matching effect in a Λ-type laser system. Two quasimonochromatic fields are directly generated by two lasing transitions, and the coherence between two laser fields can well exceed either laser linewidth. This result denotes that although either laser field has a high phase fluctuation, two field phases can match each other. Additionally, since the quantum phase-matching effect discussed here is based on the stimulated emission, the higher laser intensities lead to a higher coherence between two laser fields, which is contrary to the result in Ref. [17].

The Λ-type laser system has been extensively studied in connection with the lasing without inversion (LWI) [19–21]. A lasing field couples one of the atomic transitions, while

*dsyu@amo.t.u-tokyo.ac.jp

†jbchen@pku.edu.cn

an external driving field is tuned close to the resonance with another atomic transition. Driving and lasing fields can interact via the coherence generated on the remaining uncoupled transition. The major idea is to suppress the resonant absorption at the lasing transition due to the interference of two difference channels. On the other hand, many of the proposals and theoretical analyses of LWI deal with the preparation of macroscopic coherence between some of the low-lying atomic states [22], which is generated by a microwave field [23].

Our discussion is completely based on the standard quantum Langevin approach [24–27]. In Sec. II, we derive the basic Heisenberg-Langevin equations for the single-atom and macroscopic atomic variables and convert the quantum Langevin equations into c-number stochastic differential equations. In Sec. III, we list the steady-state solutions of laser systems in different lasing cases. In Sec. IV, we investigate the stability of the steady-state solutions based on the standard linear stability analysis. We also discuss the non-Markovian behavior of phase fluctuations, laser linewidths, and linewidth of the frequency-difference wave of two laser fields. In Sec. V, we use the Nd:YAG laser as an example to specifically discuss this phase-matching effect. In Sec. VI, we calculate the spectrum of amplitude fluctuations of fields outside the cavity. Finally, our conclusion is summarized in Sec. VII. All the diffusion coefficients for the single and macroscopic atomic Langevin noise operators and for the c-number Langevin noise variables are listed in the Appendix.

II. QUANTUM LANGEVIN EQUATIONS

A. Physical model

Here we consider the laser system shown in Fig. 1. Atoms with a Λ-type structure fly into a ring cavity. We assume that the cross section of the laser beam is so wide (or the speed of atom is so slow) that the atom-field interaction time is only determined by the lifetime of atomic levels, not the atomic transit time. In this case, it is unnecessary to consider the influence of finite atom-field interaction time on the field coherence. Additionally, we assume that the transmission direction of atomic movement is perpendicular to the transmission direction of laser fields. Thus, what we consider here is a homogeneously broadened laser system. Two lasing transitions $|c\rangle \leftrightarrow |a\rangle$ (frequency ω_{ca}) and $|c\rangle \leftrightarrow |b\rangle$ (frequency ω_{cb}) couple to different cavity modes (frequencies ω_{La} and ω_{Lb}) with detunings $\delta_a = \omega_{La} - \omega_{ca}$ and $\delta_b = \omega_{Lb} - \omega_{cb}$, respectively.

Before entering the cavity, all atoms are pumped into the upper lasing state $|c\rangle$. γ_{ca} and γ_{cb} are the spontaneous decay rates of transitions $|c\rangle \leftrightarrow |a\rangle$ and $|c\rangle \leftrightarrow |b\rangle$; γ_a, γ_b, and γ_c' are the decay rates of atoms on levels $|a,b,c\rangle$ to other atomic states; and Γ_A, Γ_B, and Γ_C are the damping rates of atomic polarizations, which obey the inequalities $2\Gamma_A \geqslant \gamma_{ca} + \gamma_{cb} + \gamma_c' + \gamma_a$, $2\Gamma_B \geqslant \gamma_{ca} + \gamma_{cb} + \gamma_c' + \gamma_b$, and $2\Gamma_C \geqslant \gamma_a + \gamma_b$. Here we do not need to consider the spontaneous decay rate of the transition $|a\rangle \leftrightarrow |b\rangle$ since for the usual laser system it is forbidden to transition between $|a\rangle$ and $|b\rangle$.

Here we should note that laser system with a Λ-type configuration like that shown in Fig. 1 can be widely found in nature, for example, He-Ne lasers, CO_2 lasers, and argon lasers. In this case, the physical model considered here is quite a universal system.

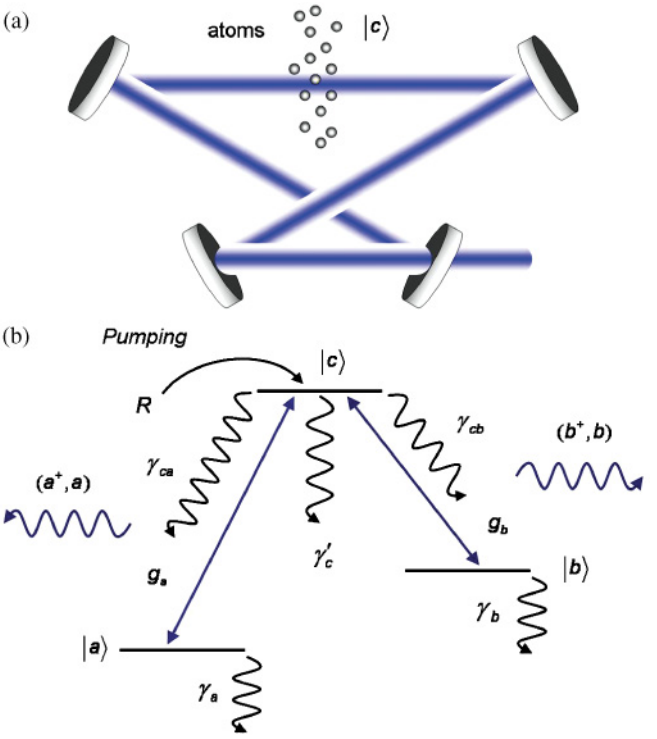

FIG. 1. (Color online) (a) Scheme of a general laser system. Atoms with a Λ-type configuration fly into a ring cavity, which couples to both two lasing transitions. (b) Relevant atomic levels. The pumping rate of the upper lasing level is R. The atom-cavity coupling strengths of two lasing transitions are g_a and g_b, respectively.

B. Quantum Langevin equations for fields interacting with single atom

In the interaction picture with the rotating wave approximation, the Hamiltonian of the laser system shown in Fig. 1 is given by

$$H = \hbar g_a \sum_j \theta(t - t_j)\left(a^\dagger \sigma_A^j e^{i\delta_a t} + \sigma_A^{j+} a e^{-i\delta_a t}\right) + \hbar g_b \sum_j \theta(t - t_j)\left(b^\dagger \sigma_B^j e^{i\delta_b t} + \sigma_B^{j+} b e^{-i\delta_b t}\right), \quad (2)$$

where a ($a^\dagger$) and b ($b^\dagger$) are the annihilation (creation) operators for the electromagnetic fields. σ_A^j and σ_B^j are the atomic polarization operators $(|a\rangle\langle c|)^j$ and $(|b\rangle\langle c|)^j$ for the jth atom. $\theta(t)$ is the unit step function [$\theta(t) = 1$ for $t > 0$, $\theta(t) = 1/2$ for $t = 0$, and $\theta(t) = 0$ for $t < 0$]. From this interaction Hamiltonian, one can find the following quantum Langevin equations of fields and atomic operators:

$$\dot{a}(t) = -\frac{\kappa_a}{2} a(t) - i g_a \sum_j \theta(t - t_j)\sigma_A^j(t) + F_{\kappa a}(t), \quad (3)$$

$$\dot{b}(t) = -\frac{\kappa_b}{2} b(t) - i g_b \sum_j \theta(t - t_j)\sigma_B^j(t) + F_{\kappa b}(t), \quad (4)$$

$$\dot{\sigma}^j_{aa}(t) = \gamma_{ca}\sigma^j_{cc}(t) - \gamma_a\sigma^j_{aa}(t) + ig_a\theta(t-t_j) \times \left[\sigma^{j+}_A(t)a(t) - a^\dagger(t)\sigma^j_A(t)\right] + f^j_{aa}(t), \quad (5)$$

$$\dot{\sigma}^j_{bb}(t) = \gamma_{cb}\sigma^j_{cc}(t) - \gamma_b\sigma^j_{bb}(t) + ig_b\theta(t-t_j) \times \left[\sigma^{j+}_B(t)b(t) - b^\dagger(t)\sigma^j_B(t)\right] + f^j_{bb}(t), \quad (6)$$

$$\dot{\sigma}^j_{cc}(t) = -(\gamma_{ca}+\gamma_{cb}+\gamma'_c)\sigma^j_{cc}(t) - ig_a\theta(t-t_j) \times \left[\sigma^{j+}_A(t)a(t) - a^\dagger(t)\sigma^j_A(t)\right] - ig_b\theta(t-t_j) \times \left[\sigma^{j+}_B(t)b(t) - b^\dagger(t)\sigma^j_B(t)\right] + f^j_{cc}(t), \quad (7)$$

$$\dot{\sigma}^j_A(t) = -(\Gamma_A - i\delta_a)\sigma^j_A(t) - ig_b\theta(t-t_j)\sigma^j_C(t)b(t) + ig_a\theta(t-t_j)\left[\sigma^j_{cc}(t) - \sigma^j_{aa}(t)\right]a(t) + f^j_A(t), \quad (8)$$

$$\dot{\sigma}^j_B(t) = -(\Gamma_B - i\delta_b)\sigma^j_B(t) - ig_a\theta(t-t_j)\sigma^{j+}_C(t)a(t) + ig_b\theta(t-t_j)\left[\sigma^j_{cc}(t) - \sigma^j_{bb}(t)\right]b(t) + f^j_B(t), \quad (9)$$

$$\dot{\sigma}^j_C(t) = -[\Gamma_C - i(\delta_a-\delta_b)]\sigma^j_C(t) + i\theta(t-t_j) \times \left[g_a\sigma^{j+}_B(t)a(t) - g_b b^\dagger(t)\sigma^j_A(t)\right] + f^j_C(t), \quad (10)$$

where the single-atom operators for the jth atom are defined as $\sigma^j_{aa} = (|a\rangle\langle a|)^j$, $\sigma^j_{bb} = (|b\rangle\langle b|)^j$, $\sigma^j_{cc} = (|c\rangle\langle c|)^j$, $\sigma^j_C = (|a\rangle\langle b|)^j$, $\sigma^{j+}_A = (|c\rangle\langle a|)^j$, $\sigma^{j+}_B = (|c\rangle\langle b|)^j$, and $\sigma^{j+}_C = (|b\rangle\langle a|)^j$. The cavity loss $\kappa_{a,b}$ and atomic decay are modeled in the standard way by coupling the radiation fields and each atom to heat reservoirs. The above Heisenberg-Langevin equations have the same structure,

$$\dot{x}(t) = A_x(t) + f_x(t), \quad (11)$$

where $A_x(t)$ is the deterministic part of the equation and $f_x(t)$ is the quantum noise operator. The noise operators for the single-atom variables are δ correlated in time,

$$\left\langle f^i_x(t) f^j_y(t')\right\rangle = \mathfrak{d}(x,y)\delta_{i,j}\,\delta(t-t'), \quad (12)$$

where $\mathfrak{d}(x,y)$ is the diffusion coefficient. $\delta_{i,j}$ makes only correlations between noise operators corresponding to the same atom be nonzero. Using the generalized dissipation-fluctuation theorem,

$$\mathfrak{d}(x,y) = -\langle xA_y\rangle - \langle A_x y\rangle + \frac{d}{dt}\langle xy\rangle, \quad (13)$$

one can calculate the diffusion coefficients. The nonvanishing terms are listed in the Appendix. For the field Langevin force $F_{\kappa\alpha}(t)$, one gets $\langle F_{\kappa\alpha}(t)\rangle = 0$, and

$$\langle F^+_{\kappa\alpha}(t)F_{\kappa\beta}(t')\rangle = \kappa_\alpha n_{\rm th}\delta_{\alpha,\beta}\delta(t-t'), \quad (14)$$

$$\langle F_{\kappa\alpha}(t)F^+_{\kappa\beta}(t')\rangle = \kappa_\alpha(n_{\rm th}+1)\delta_{\alpha,\beta}\delta(t-t'), \quad (15)$$

$$\langle F_{\kappa\alpha}(t)F_{\kappa\beta}(t')\rangle = 0, \quad (16)$$

$$\langle F^+_{\kappa\alpha}(t)F^+_{\kappa\beta}(t')\rangle = 0, \quad (17)$$

where $n_{\rm th}$ is the temperature-dependent mean thermal photon number and $\alpha,\beta = a,b$.

C. Quantum Langevin equations for fields interacting with macroscopic atoms

The macroscopic atomic operators can be defined by adding up all the individual atomic operators and taking into account the corresponding injection times into the cavity. Then, we have

$$N_{aa}(t) = \sum_j \theta(t-t_j)\sigma^j_{aa}(t), \quad (18)$$

$$N_{bb}(t) = \sum_j \theta(t-t_j)\sigma^j_{bb}(t), \quad (19)$$

$$N_{cc}(t) = \sum_j \theta(t-t_j)\sigma^j_{cc}(t), \quad (20)$$

$$M_A(t) = -i\sum_j \theta(t-t_j)\sigma^j_A(t), \quad (21)$$

$$M_B(t) = -i\sum_j \theta(t-t_j)\sigma^j_B(t), \quad (22)$$

$$M_C(t) = \sum_j \theta(t-t_j)\sigma^j_C(t). \quad (23)$$

The additional factor $(-i)$ is introduced for mathematical convenience. Operators $M_A(t)$, $M_B(t)$, and $M_C(t)$ represent the macroscopic atomic polarizations, and $N_{aa}(t)$, $N_{bb}(t)$, and $N_{cc}(t)$ represent the macroscopic populations of levels $|a,b,c\rangle$, respectively. With the aforementioned definitions and Eqs. (3)–(10), the quantum Langevin equations for the electromagnetic fields and macroscopic atomic operators can be expressed as

$$\dot{a}(t) = -\frac{\kappa_a}{2}a(t) + g_a M_A(t) + F_{\kappa a}(t), \quad (24)$$

$$\dot{b}(t) = -\frac{\kappa_b}{2}b(t) + g_b M_B(t) + F_{\kappa b}(t), \quad (25)$$

$$\dot{N}_{aa}(t) = \gamma_{ca}N_{cc}(t) - \gamma_a N_{aa}(t) + g_a[M^+_A(t)a(t) + a^\dagger(t)M_A(t)] + F_{aa}(t), \quad (26)$$

$$\dot{N}_{bb}(t) = \gamma_{cb}N_{cc}(t) - \gamma_b N_{bb}(t) + g_b[M^+_B(t)b(t) + b^\dagger(t)M_B(t)] + F_{bb}(t), \quad (27)$$

$$\dot{N}_{cc}(t) = R - (\gamma_{ca}+\gamma_{cb}+\gamma'_c)N_{cc}(t) - g_a[M^+_A(t)a(t) + a^\dagger(t)M_A(t)] - g_b[M^+_B(t)b(t) + b^\dagger(t)M_B(t)] + F_{cc}(t), \quad (28)$$

$$\dot{M}_A(t) = -(\Gamma_A - i\delta_a)M_A(t) - g_b M_C(t)b(t) + g_a[N_{cc}(t) - N_{aa}(t)]a(t) + F_A(t), \quad (29)$$

$$\dot{M}_B(t) = -(\Gamma_B - i\delta_b)M_B(t) - g_a M^+_C(t)a(t) + g_b[N_{cc}(t) - N_{bb}(t)]b(t) + F_B(t), \quad (30)$$

$$\dot{M}_C(t) = -[\Gamma_C - i(\delta_a-\delta_b)]M_C(t) + g_a M^+_B(t)a(t) + g_b b^\dagger(t)M_A(t) + F_C(t), \quad (31)$$

where the total noise operators for the macroscopic atomic operators are given by

$$F_{aa}(t) = \sum_j\left[\delta(t-t_j)\sigma^j_{aa}(t_j) + \theta(t-t_j)f^j_{aa}(t)\right], \quad (32)$$

$$F_{bb}(t) = \sum_j\left[\delta(t-t_j)\sigma^j_{bb}(t_j) + \theta(t-t_j)f^j_{bb}(t)\right], \quad (33)$$

$$F_{cc}(t) = \sum_j\left[\delta(t-t_j)\sigma^j_{cc}(t_j) + \theta(t-t_j)f^j_{cc}(t)\right] - R, \quad (34)$$

$$F_A(t) = -i\sum_j\left[\delta(t-t_j)\sigma^j_A(t_j) + \theta(t-t_j)f^j_A(t)\right], \quad (35)$$

$$F_B(t) = -i\sum_j \left[\delta(t-t_j)\sigma_B^j(t_j) + \theta(t-t_j)f_B^j(t)\right], \quad (36)$$

$$F_C(t) = \sum_j \left[\delta(t-t_j)\sigma_C^j(t_j) + \theta(t-t_j)f_C^j(t)\right], \quad (37)$$

and the average of each macroscopic noise operator is zero. In deriving these macroscopic noise operators, we have used

$$\langle \delta(t-t_j)\rangle_S = R\int_{-\infty}^{+\infty} dt_j\, \delta(t-t_j) = R, \quad (38)$$

where R is the mean pumping rate and $\langle\cdots\rangle_S$ denotes the classical average over the injection times and the fact that each atom was on the upper lasing state $|c\rangle$ at its injection time. The correlation function between two quantum Langevin forces $F_\alpha(t)$ and $F_\beta(t)$ can be expressed as

$$\langle F_\alpha(t)F_\beta(t')\rangle = \mathfrak{D}(\alpha,\beta)\delta(t-t'), \quad (39)$$

where the nonvanishing diffusion coefficients $\mathfrak{D}(\alpha,\beta)$ are listed in the Appendix.

D. Equivalent *c*-number stochastic Langevin equations for a normally ordered product of operators

Now we derive the stochastic c-number Langevin equations, which are equivalent to the quantum Langevin equations. For this we should choose some particular ordering for the products of atomic and field operators, because the c-number variables commute with each other while the operators do not. Here we choose the normal ordering of atomic and field operators, that is, $a^\dagger(t)$, $b^\dagger(t)$, $M_A^+(t)$, $M_B^+(t)$, $M_C^+(t)$, $N_{aa}(t)$, $N_{bb}(t)$, $N_{cc}(t)$, $M_C(t)$, $M_B(t)$, $M_A(t)$, $b(t)$, and $a(t)$. The stochastic c-number variables corresponding to the operators $a(t)$, $b(t)$, $M_A(t)$, $M_B(t)$, $M_C(t)$, $N_{aa}(t)$, $N_{bb}(t)$, and $N_{cc}(t)$ are denoted by $\mathcal{A}(t)$, $\mathcal{B}(t)$, $\mathcal{M}_A(t)$, $\mathcal{M}_B(t)$, $\mathcal{M}_C(t)$, $\mathcal{N}_{aa}(t)$, $\mathcal{N}_{bb}(t)$, and $\mathcal{N}_{cc}(t)$, respectively. Equations (24)–(31) are already written in normal order, and one can directly obtain the equations for the corresponding c-number variables,

$$\dot{\mathcal{A}}(t) = -\frac{\kappa_a}{2}\mathcal{A}(t) + g_a\mathcal{M}_A(t) + \mathcal{F}_{\kappa a}(t), \quad (40)$$

$$\dot{\mathcal{B}}(t) = -\frac{\kappa_b}{2}\mathcal{B}(t) + g_b\mathcal{M}_B(t) + \mathcal{F}_{\kappa b}(t), \quad (41)$$

$$\dot{\mathcal{N}}_{aa}(t) = \gamma_{ca}\mathcal{N}_{cc}(t) - \gamma_a\mathcal{N}_{aa}(t) + g_a[\mathcal{M}_A^*(t)\mathcal{A}(t) + \mathcal{A}^*(t)\mathcal{M}_A(t)] + \mathcal{F}_{aa}(t), \quad (42)$$

$$\dot{\mathcal{N}}_{bb}(t) = \gamma_{cb}\mathcal{N}_{cc}(t) - \gamma_b\mathcal{N}_{bb}(t) + g_b[\mathcal{M}_B^*(t)\mathcal{B}(t) + \mathcal{B}^*(t)\mathcal{M}_B(t)] + \mathcal{F}_{bb}(t), \quad (43)$$

$$\dot{\mathcal{N}}_{cc}(t) = R - (\gamma_{ca}+\gamma_{cb}+\gamma_c')\mathcal{N}_{cc}(t) - g_a[\mathcal{M}_A^*(t)\mathcal{A}(t) + \mathcal{A}^*(t)\mathcal{M}_A(t)] - g_b[\mathcal{M}_B^*(t)\mathcal{B}(t) + \mathcal{B}^*(t)\mathcal{M}_B(t)] + \mathcal{F}_{cc}(t), \quad (44)$$

$$\dot{\mathcal{M}}_A(t) = -(\Gamma_A - i\delta_a)\mathcal{M}_A(t) - g_b\mathcal{M}_C(t)\mathcal{B}(t) + g_a[\mathcal{N}_{cc}(t) - \mathcal{N}_{aa}(t)]\mathcal{A}(t) + \mathcal{F}_A(t), \quad (45)$$

$$\dot{\mathcal{M}}_B(t) = -(\Gamma_B - i\delta_b)\mathcal{M}_B(t) - g_a\mathcal{M}_C^*(t)\mathcal{A}(t) + g_b[\mathcal{N}_{cc}(t) - \mathcal{N}_{bb}(t)]\mathcal{B}(t) + \mathcal{F}_B(t), \quad (46)$$

$$\dot{\mathcal{M}}_C(t) = -[\Gamma_C - i(\delta_a-\delta_b)]\mathcal{M}_C(t) + g_a\mathcal{M}_B^*(t)\mathcal{A}(t) + g_b\mathcal{B}^*(t)\mathcal{M}_A(t) + \mathcal{F}_C(t). \quad (47)$$

The stochastic c-number Langevin forces of the corresponding quantum noise operators are denoted by $\mathcal{F}_\mu(t)$ with $\mu = \kappa a$, κb, A, B, C, aa, bb, and cc, and we have the properties $\langle\mathcal{F}_\mu(t)\rangle = 0$ and

$$\langle\mathcal{F}_\mu(t)\mathcal{F}_\nu(t')\rangle = \mathcal{D}_{\mu\nu}\delta(t-t'). \quad (48)$$

The c-number diffusion coefficients $\mathcal{D}_{\mu\nu}$ can be obtained from the quantum diffusion coefficients by transforming the expressions in the fluctuation-dissipation theorem of Eq. (13) into the normally ordered operator products. If $\hat{x}\hat{y}$ is normally ordered, its expectation value is equal to the expectation value of the corresponding c-number product. Hence, we have

$$\frac{d}{dt}\langle\hat{x}\hat{y}\rangle = \frac{d}{dt}\langle xy\rangle. \quad (49)$$

Using again the generalized dissipation-fluctuation theorem, we find that

$$\mathcal{D}_{xy} = \mathfrak{D}_{xy} + \langle\hat{x}\hat{A}_y\rangle + \langle\hat{A}_x\hat{y}\rangle - \langle xA_y\rangle - \langle A_x y\rangle. \quad (50)$$

All the nonvanishing c-number diffusion coefficients are listed in the Appendix.

III. STEADY-STATE SOLUTION

The steady-state solution for the mean values of the fields and atomic variables can be obtained from the c-number dynamics equations. For the sake of simplicity, we only consider the resonant case $\delta_a = \delta_b = 0$. In this case, the optical phases are randomly distributed between 0 and 2π in the stationary state. We can choose the arbitrary mean values of the optical phases to be zero, which is quite convenient since then all the atomic polarizations $\mathcal{M}_{A0}$, $\mathcal{M}_{B0}$, and $\mathcal{M}_{C0}$ become real. The subscript 0 denotes the stationary solution. The atomic cooperativity parameters corresponding to two lasing transitions $|c\rangle$-$|a\rangle$ and $|c\rangle$-$|b\rangle$ are defined as

$$\mathcal{C}_a \equiv \frac{2g_a^2}{\Gamma_A\kappa_a}, \quad \mathcal{C}_b \equiv \frac{2g_b^2}{\Gamma_B\kappa_b},$$

respectively, and the photon numbers inside the cavity are given by $\mathcal{I}_{a0} = \mathcal{A}_0^2$ and $\mathcal{I}_{b0} = \mathcal{B}_0^2$. The steady-state values of the field amplitudes are completely determined by the atomic polarizations as $\mathcal{A}_0 = \frac{2g_a}{\kappa_a}\mathcal{M}_{A0}$ and $\mathcal{B}_0 = \frac{2g_b}{\kappa_b}\mathcal{M}_{B0}$. On the other hand, the pumping rate R should be equal to the loss rate of the atomic population,

$$\gamma_a\mathcal{N}_{aa0} + \gamma_b\mathcal{N}_{bb0} + \gamma_c'\mathcal{N}_{cc0} = R. \quad (51)$$

We have two possible cases of laser production: (i) The pumping rate is so weak that only one lasing transition realizes the optical oscillation inside the cavity. (ii) Both laser oscillations are realized for a high pumping rate.

A. $\mathcal{A}_0 \neq 0$ and $\mathcal{B}_0 = 0$

In this special case, only the optical field based on the lasing transition $|c\rangle$-$|a\rangle$ is oscillating inside the cavity and we have the photon number $\mathcal{I}_{a0}$ of field $\mathcal{A}_0$,

$$\mathcal{I}_{a0}^{(a,0)} = \frac{1}{(\bar{\gamma}_a/\gamma_a)+1}\frac{R-\bar{\gamma}_a/\mathcal{C}_a}{\kappa_a}, \quad (52)$$

and the populations of levels $|a,b,c\rangle$,

$$\mathcal{N}_{aa0}^{(a,0)} = \frac{R-(\gamma_c'+\gamma_{cb})/\mathcal{C}_a}{\gamma_c'+\gamma_{cb}+\gamma_a}, \quad (53)$$

$$\mathcal{N}_{bb0}^{(a,0)} = \frac{\gamma_{cb}}{\gamma_b}\frac{R+\gamma_a/\mathcal{C}_a}{\gamma_c'+\gamma_{cb}+\gamma_a}, \tag{54}$$

$$\mathcal{N}_{cc0}^{(a,0)} = \frac{R+\gamma_a/\mathcal{C}_a}{\gamma_c'+\gamma_{cb}+\gamma_a}, \tag{55}$$

where $\bar{\gamma}_a = \gamma_a\gamma_{ct}/(\gamma_a-\gamma_{ca})$ is the effective decay rate, and $\gamma_{ct} \equiv \gamma_c' + \gamma_{cb} + \gamma_{ca}$ is the total damping rate of level $|c\rangle$. Here we use the superscript $(a,0)$ to denote the case of $\mathcal{A}_0 \neq 0$ and $\mathcal{B}_0 = 0$. From Eq. (52) we have the saturation intensity of the laser field $\mathcal{I}_{a0}^{(0)}$,

$$\mathcal{I}_{as}^{(a,0)} = \frac{\gamma_a\bar{\gamma}_a}{\gamma_a+\bar{\gamma}_a}\frac{\Gamma_A}{2g_A^2}, \tag{56}$$

and the threshold of the pumping rate $R_{\rm TH}^{(a,0)} = \bar{\gamma}_a/\mathcal{C}_a$. It is easy to derive the necessary condition for laser oscillation: $\gamma_a > \gamma_{ca}$. When $R \gg R_{\rm TH}$ and $\mathcal{I}_{a0}^{(a,0)} \gg \mathcal{I}_{as}^{(a,0)}$, the populations of levels $|a\rangle$ and $|c\rangle$ approach each other and the inversion goes to zero, corresponding to saturation.

B. $\mathcal{A}_0 = 0$ and $\mathcal{B}_0 \neq 0$

Similarly, for the case of $\mathcal{A}_0 = 0$ we have the photon number $\mathcal{I}_{b0}$ of field $\mathcal{B}_0$,

$$\mathcal{I}_{b0}^{(b,0)} = \frac{1}{(\bar{\gamma}_b/\gamma_b)+1}\frac{R-\bar{\gamma}_b/\mathcal{C}_b}{\kappa_b}, \tag{57}$$

and the populations of three levels

$$\mathcal{N}_{aa0}^{(b,0)} = \frac{\gamma_{ca}}{\gamma_a}\frac{R+\gamma_b/\mathcal{C}_b}{\gamma_c'+\gamma_{ca}+\gamma_b}, \tag{58}$$

$$\mathcal{N}_{bb0}^{(b,0)} = \frac{R-(\gamma_c'+\gamma_{ca})/\mathcal{C}_b}{\gamma_c'+\gamma_{ca}+\gamma_b}, \tag{59}$$

$$\mathcal{N}_{cc0}^{(b,0)} = \frac{R+\gamma_b/\mathcal{C}_b}{\gamma_c'+\gamma_{ca}+\gamma_b}, \tag{60}$$

where $\bar{\gamma}_b = \gamma_b\gamma_{ct}/(\gamma_b-\gamma_{cb})$ is the effective decay rate. The saturation intensity of the laser field $\mathcal{I}_{b0}^{(b,0)}$ is given by

$$\mathcal{I}_{bs}^{(b,0)} = \frac{\gamma_b\bar{\gamma}_b}{\gamma_b+\bar{\gamma}_b}\frac{\Gamma_B}{2g_B^2}, \tag{61}$$

and the threshold pumping rate is $R_{\rm TH}^{(b,0)} = \bar{\gamma}_b/\mathcal{C}_b$. We use the superscript $(b,0)$ to denote the case of $\mathcal{A}_0 = 0$ and $\mathcal{B}_0 \neq 0$. Comparing two thresholds $R_{\rm TH}^{(a,0)}$ and $R_{\rm TH}^{(b,0)}$, when the pumping rate R increases from zero, laser field $\mathcal{A}_0$ ($\mathcal{B}_0$) starts oscillating prior to field $\mathcal{B}_0$ ($\mathcal{A}_0$) for $R_{\rm TH}^{(a,0)} < R_{\rm TH}^{(b,0)}$ ($R_{\rm TH}^{(a,0)} > R_{\rm TH}^{(b,0)}$).

C. $\mathcal{A}_0 \neq 0$ and $\mathcal{B}_0 \neq 0$

For the case of two laser fields oscillating, we have the photon numbers inside the cavity,

$$\mathcal{I}_{a0}^{(1)} = \frac{\left[(R/\bar{\gamma}_a)-\mathcal{C}_a^{-1}\right]q_b - \left[(R/\bar{\gamma}_b)-\mathcal{C}_b^{-1}\right]p_b}{q_aq_b - p_ap_b}, \tag{62}$$

$$\mathcal{I}_{b0}^{(1)} = \frac{\left[(R/\bar{\gamma}_b)-\mathcal{C}_b^{-1}\right]q_a - \left[(R/\bar{\gamma}_a)-\mathcal{C}_a^{-1}\right]p_a}{q_aq_b - p_ap_b}, \tag{63}$$

based on which, the populations of three levels can be expressed as

$$\mathcal{N}_{aa0}^{(1)} = \frac{\gamma_{ca}}{\gamma_a\gamma_{ct}}\left[R+\left(\frac{\gamma_{ct}}{\gamma_{ca}}-1\right)\kappa_a\mathcal{I}_{a0}^{(1)} - \kappa_b\mathcal{I}_{b0}^{(1)}\right], \tag{64}$$

$$\mathcal{N}_{bb0}^{(1)} = \frac{\gamma_{cb}}{\gamma_b\gamma_{ct}}\left[R-\kappa_a\mathcal{I}_{a0}^{(1)}+\left(\frac{\gamma_{ct}}{\gamma_{cb}}-1\right)\kappa_b\mathcal{I}_{b0}^{(1)}\right], \tag{65}$$

$$\mathcal{N}_{cc0}^{(1)} = \frac{1}{\gamma_c'}\left(R-\gamma_a\mathcal{N}_{aa0}^{(1)}-\gamma_b\mathcal{N}_{bb0}^{(1)}\right). \tag{66}$$

The superscript (1) denotes the case of $\mathcal{A}_0 \neq 0$ and $\mathcal{B}_0 \neq 0$. The parameters in the above equations are defined as $q_a = \kappa_a(\gamma_a^{-1}+\bar{\gamma}_a^{-1})$, $q_b = \kappa_b(\gamma_b^{-1}+\bar{\gamma}_b^{-1})$, $p_a = (\kappa_a/\bar{\gamma}_b)+(g_a/g_b)\mathcal{Q}$, $p_b = (\kappa_b/\bar{\gamma}_a)+(g_b/g_a)\mathcal{Q}$, and $\mathcal{Q} = \frac{1}{\Gamma_C}\left(\frac{g_a\kappa_b}{2g_b}+\frac{g_b\kappa_a}{2g_a}\right)$.

As we have pointed out, for the case of $R_{\rm TH}^{(a,0)} < R_{\rm TH}^{(b,0)}$, laser field $\mathcal{A}_0$ starts oscillating prior to field $\mathcal{B}_0$ when the pumping rate R increases from zero, and then field $\mathcal{B}_0$ starts to oscillate when

$$R > R_{\rm TH}^{(b,1)} \equiv \frac{(q_a/\mathcal{C}_b)-(p_a/\mathcal{C}_a)}{(q_a/\bar{\gamma}_b)-(p_a/\bar{\gamma}_a)}, \tag{67}$$

which is derived from the condition of $\mathcal{I}_{b0}^{(b,0)} = \mathcal{I}_{b0}^{(1)}$. Contrarily, for the case of $R_{\rm TH}^{(a,0)} > R_{\rm TH}^{(b,0)}$, laser field $\mathcal{A}_0$ starts to oscillate when

$$R > R_{\rm TH}^{(a,1)} \equiv \frac{(q_b/\mathcal{C}_a)-(p_b/\mathcal{C}_b)}{(q_b/\bar{\gamma}_a)-(p_b/\bar{\gamma}_b)}, \tag{68}$$

which can be derived from the condition of $\mathcal{I}_{a0}^{(a,0)} = \mathcal{I}_{a0}^{(1)}$. Figure 2 displays the phase diagram of a Λ-type laser system. There is a point corresponding to $R_{\rm TH}^{(a,0)} = R_{\rm TH}^{(b,0)} = R_{\rm TH}^{(a,1)} = R_{\rm TH}^{(b,1)}$, at which two laser fields simultaneously start to oscillate. From Eqs. (67) and (68) one can see that when $(q_a/\bar{\gamma}_b) \sim (p_a/\bar{\gamma}_a)$ [or $(q_b/\bar{\gamma}_a) \sim (p_b/\bar{\gamma}_b)$], the threshold $R_{\rm TH}^{(b,1)}$ (or $R_{\rm TH}^{(a,1)}$) for two fields oscillating approaches infinity, which

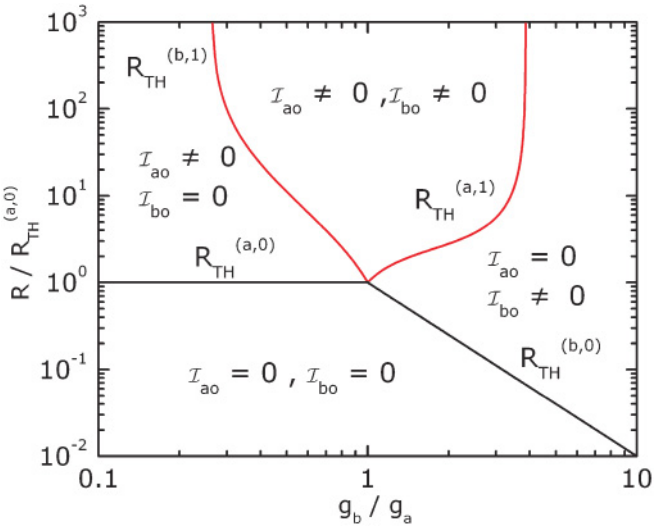

FIG. 2. (Color online) Phase diagram of laser system. Use $R_{\rm TH}^{(a,0)}$ as the unit of pumping rate, and frequency is given in units of g_a. For all curves $\kappa_a = \kappa_b = 5\times10^3$, $\gamma_a = \gamma_b = 5\times10^4$, $\gamma_c' = \gamma_{ca} = \gamma_{cb} = 10^4$, $\Gamma_A = \Gamma_B = 5\times10^4$, and $\Gamma_C = 4\times10^5$. The solid lines denote the boundaries of different oscillating cases.

denotes that only one laser field can oscillate inside the cavity even for a high pumping rate. Additionally, one can see that two laser fields oscillating only happens when two atom-cavity coupling constants $g_{a,b}$ are close to each other.

IV. QUANTUM FLUCTUATIONS OF THE LASER FIELDS AROUND STEADY STATES

To investigate the small fluctuations of the laser fields and atomic variables around steady states we consider all the variables, as usual, as the sum of the steady-state solution and a small fluctuating term. For example, for $\mathcal{N}_{aa}(t)$ we set $\mathcal{N}_{aa}(t) = \mathcal{N}_{aa0} + \delta\mathcal{N}_{aa}(t)$ and in the same way for the other variables. It should be assumed that the laser system is operating sufficiently above threshold so that the fluctuations of dynamic variables are much smaller than their steady-state values. Based on Eqs. (40)–(47), one can obtain a set of linear equations in the resonant case

$$\delta\dot{\mathcal{A}}(t) = -\frac{\kappa_a}{2}\delta\mathcal{A}(t) + g_a\delta\mathcal{M}_A(t) + \mathcal{F}_{\kappa a}(t), \tag{69}$$

$$\delta\dot{\mathcal{B}}(t) = -\frac{\kappa_b}{2}\delta\mathcal{B}(t) + g_b\delta\mathcal{M}_B(t) + \mathcal{F}_{\kappa b}(t), \tag{70}$$

$$\begin{aligned}\delta\dot{\mathcal{N}}_{aa}(t) = {}& \gamma_{ca}\delta\mathcal{N}_{cc}(t) - \gamma_a\delta\mathcal{N}_{aa}(t) \\ & + g_a\mathcal{A}_0[\delta\mathcal{M}_A^*(t) + \delta\mathcal{M}_A(t)] \\ & + g_a\mathcal{M}_{A0}[\delta\mathcal{A}^*(t) + \delta\mathcal{A}(t)] + \mathcal{F}_{aa}(t),\end{aligned} \tag{71}$$

$$\begin{aligned}\delta\dot{\mathcal{N}}_{bb}(t) = {}& \gamma_{cb}\delta\mathcal{N}_{cc}(t) - \gamma_b\delta\mathcal{N}_{bb}(t) \\ & + g_b\mathcal{B}_0[\delta\mathcal{M}_B^*(t) + \delta\mathcal{M}_B(t)] \\ & + g_b\mathcal{M}_{B0}[\delta\mathcal{B}^*(t) + \delta\mathcal{B}(t)] + \mathcal{F}_{bb}(t),\end{aligned} \tag{72}$$

$$\begin{aligned}\delta\dot{\mathcal{N}}_{cc}(t) = {}& -(\gamma_c' + \gamma_{cb} + \gamma_{ca})\delta\mathcal{N}_{cc}(t) - g_a\mathcal{A}_0[\delta\mathcal{M}_A^*(t) \\ & + \delta\mathcal{M}_A(t)] - g_a\mathcal{M}_{A0}[\delta\mathcal{A}^*(t) + \delta\mathcal{A}(t)] \\ & - g_b\mathcal{B}_0[\delta\mathcal{M}_B^*(t) + \delta\mathcal{M}_B(t)] - g_b\mathcal{M}_{B0}[\delta\mathcal{B}^*(t) \\ & + \delta\mathcal{B}(t)] + \mathcal{F}_{cc}(t),\end{aligned} \tag{73}$$

$$\begin{aligned}\delta\dot{\mathcal{M}}_A(t) = {}& -\Gamma_A\delta\mathcal{M}_A(t) + g_a(\mathcal{N}_{cc0} - \mathcal{N}_{aa0})\delta\mathcal{A}(t) \\ & + g_a\mathcal{A}_0[\delta\mathcal{N}_{cc}(t) - \delta\mathcal{N}_{aa}(t)] - g_b\mathcal{B}_0\delta\mathcal{M}_C(t) \\ & - g_b\mathcal{M}_{C0}\delta\mathcal{B}(t) + \mathcal{F}_A(t),\end{aligned} \tag{74}$$

$$\begin{aligned}\delta\dot{\mathcal{M}}_B(t) = {}& -\Gamma_B\delta\mathcal{M}_B(t) + g_b(\mathcal{N}_{cc0} - \mathcal{N}_{bb0})\delta\mathcal{B}(t) \\ & + g_b\mathcal{B}_0[\delta\mathcal{N}_{cc}(t) - \delta\mathcal{N}_{bb}(t)] - g_a\mathcal{A}_0\delta\mathcal{M}_C^*(t) \\ & - g_a\mathcal{M}_{C0}\delta\mathcal{A}(t) + \mathcal{F}_B(t),\end{aligned} \tag{75}$$

$$\begin{aligned}\delta\dot{\mathcal{M}}_C(t) = {}& -\Gamma_C\delta\mathcal{M}_C(t) + g_a\mathcal{A}_0\delta\mathcal{M}_B^*(t) + g_a\mathcal{M}_{B0}\delta\mathcal{A}(t) \\ & + g_b\mathcal{M}_{A0}\delta\mathcal{B}^*(t) + g_b\mathcal{B}_0\delta\mathcal{M}_A(t) + \mathcal{F}_C(t).\end{aligned} \tag{76}$$

Based on the above linear difference equations, we can discuss the quantum fluctuations of a laser system around steady states.

A. Linear stability analysis of the steady-state solutions

In Sec. III, we derived the steady-state solutions of Λ-type laser systems in different lasing situations. The important question is whether all of these solutions are stable for a pump rate beyond the corresponding threshold. The stability of a steady state can be analyzed by using a standard technique known as the *linear stability analysis* [28,29], which we perform next.

1. $\mathcal{A}_0 \neq 0$ and $\mathcal{B}_0 = 0$

First, let us consider the case of single field oscillating, $\mathcal{A}_0 \neq 0$ and $\mathcal{B}_0 = 0$. We begin with a trivial steady-state solution (nonlasing solution): $\mathcal{A}_0 = 0$, $\mathcal{M}_{A0} = 0$, $\mathcal{N}_{aa0} = \frac{\gamma_{ca}}{\gamma_a}\frac{R}{\gamma_{ct}}$, and $\mathcal{N}_{cc0} = \frac{R}{\gamma_{ct}}$. Based on Eqs. (69)–(76), one can easily obtain the following evolution equation of the perturbation terms:

$$\frac{d}{dt}\begin{pmatrix}\delta\mathcal{M}_A^*(t) + \delta\mathcal{M}_A(t) \\ \delta\mathcal{N}_{aa}(t) \\ \delta\mathcal{A}^*(t) + \delta\mathcal{A}(t)\end{pmatrix} = \mathbb{M}_A\begin{pmatrix}\delta\mathcal{M}_A^*(t) + \delta\mathcal{M}_A(t) \\ \delta\mathcal{N}_{aa}(t) \\ \delta\mathcal{A}^*(t) + \delta\mathcal{A}(t)\end{pmatrix},$$

where the characteristic matrix $\mathbb{M}_A$ is given by

$$\mathbb{M}_A = \begin{pmatrix}-\Gamma_A & 0 & g_a\frac{R}{\bar{\gamma}_a} \\ 0 & -\frac{\gamma_a\gamma_{ct}}{\gamma_{ct}-\gamma_{ca}} & 0 \\ g_a & 0 & -\frac{\kappa_a}{2}\end{pmatrix}. \tag{77}$$

By using the Laplace-transform technique, each fluctuation is assumed to evolve exponentially with time as e^{st}, where s is the (complex) Laplace variable. A nontrivial solution of the resulting set of algebraic equations exists only if the determinant of the coefficient matrix vanishes,

$$\det|s - \mathbb{M}_A| = 0, \tag{78}$$

which leads to the following cubic polynomial equation

$$s^3 + a_2s^2 + a_1s + a_0 = 0, \tag{79}$$

where the parameters are defined as

$$\begin{aligned}a_2 &= \Gamma_A + \frac{\kappa_a}{2} + \frac{\gamma_{ct}\gamma_a}{\gamma_{ct}-\gamma_{ca}}, \\ a_1 &= \frac{\Gamma_A\kappa_a}{2} + \frac{\gamma_{ct}\gamma_a}{\gamma_{ct}-\gamma_{ca}}\left(\Gamma_A + \frac{\kappa_a}{2}\right) - \frac{Rg_a^2}{2\bar{\gamma}_a}, \\ a_0 &= \frac{\gamma_{ct}\gamma_a}{\gamma_{ct}-\gamma_{ca}}\left(\frac{\Gamma_A\kappa_a}{2} - \frac{Rg_a^2}{2\bar{\gamma}_a}\right).\end{aligned}$$

When any solution of Eq. (79) has a positive real part, the steady state is unstable against small perturbations, since they grow exponentially with time. In fact the real part of the solution s governs the growth rate of perturbation. The critical pump value at which the steady-state solution becomes unstable is found by looking for roots of the form $s = i\Omega$. Substituting $s = i\Omega$ in Eq. (79), we obtain $a_0 = 0$ from which one can get a critical pump value $r_{\mathrm{TH,I}}^{(a,0)}$. At $r_{\mathrm{TH,I}}^{(a,0)}$ the steady state is marginally stable since the growth rate of perturbation is then zero. This pump value $r_{\mathrm{TH,I}}^{(a,0)}$ is exactly equal to $R_{\mathrm{TH}}^{(a,0)}$ and called the *first threshold* of field $\mathcal{A}_0$ in the case of single field oscillating.

Beyond the first threshold $r_{\mathrm{TH,I}}^{(a,0)}$, field $\mathcal{A}_0$ begins to oscillate inside the cavity. However, not all of the steady-state solutions for $R > r_{\mathrm{TH,I}}^{(a,0)}$ is stable. Therefore, we perform a linear stability analysis on the steady-state solutions given by

Eqs. (52)–(55). In this case, the characteristic matrix $\mathbb{M}_A$ should be reexpressed as

$$\mathbb{M}_A = \begin{pmatrix} -\Gamma_A & -2g_a\mathcal{A}_0\left(1+\frac{\gamma_a}{\gamma_{ct}-\gamma_{ca}}\right) & \frac{g_a}{\mathcal{C}_a} \\ g_a\mathcal{A}_0 & -\frac{\gamma_a\gamma_{ct}}{\gamma_{ct}-\gamma_{ca}} & g_a\mathcal{M}_{A0} \\ g_a & 0 & -\frac{\kappa_a}{2} \end{pmatrix}, \tag{80}$$

and parameters of the cubic polynomial Eq. (79) are replaced by

$$a_2 = \Gamma_A + \frac{\kappa_a}{2} + \frac{\gamma_{ct}\gamma_a}{\gamma_{ct}-\gamma_{ca}},$$
$$a_1 = \frac{\gamma_{ct}\gamma_a}{\gamma_{ct}-\gamma_{ca}}\frac{\Gamma_A\mathcal{C}_a}{\bar{\gamma}_a}\left(\bar{\gamma}_a\frac{\kappa_a^2}{4g_a^2}+R\right),$$
$$a_0 = \frac{\gamma_{ct}\gamma_a}{\gamma_{ct}-\gamma_{ca}}\frac{2g_a^2}{\bar{\gamma}_a}\left(R-\frac{\bar{\gamma}_a}{\mathcal{C}_a}\right).$$

Again, substituting $s = i\Omega$ into Eq. (79) we obtain a new critical pump rate

$$r_{\mathrm{TH,II}}^{(a,0)} = \frac{\bar{\gamma}_a}{\mathcal{C}_a}\frac{3+\frac{1}{\Gamma_A}\left(\frac{\kappa_a}{2}+\frac{\gamma_{ct}\gamma_a}{\gamma_{ct}-\gamma_{ca}}\right)}{1-\frac{2}{\kappa_a}\left(\Gamma_A+\frac{\gamma_{ct}\gamma_a}{\gamma_{ct}-\gamma_{ca}}\right)}, \tag{81}$$

beyond which the steady-state solutions (52)–(55) are no longer stable. Thus, $r_{\mathrm{TH,II}}^{(a,0)}$ is called the *instability threshold* or the *second threshold*. We note that a second threshold is not related to the atom-cavity coupling strength g_a and does not always exist. Equation (81) provides us with a necessary condition for the second threshold to exist:

$$\frac{\kappa_a}{2} > \Gamma_A + \frac{\gamma_{ct}\gamma_a}{\gamma_{ct}-\gamma_{ca}}, \tag{82}$$

which is exactly the bad-cavity condition. For the good-cavity-limit parameters chosen in Fig. 2, the second threshold $r_{\mathrm{TH,II}}^{(a,0)}$ does not exist.

2. $\mathcal{A}_0 = 0$ and $\mathcal{B}_0 \neq 0$

Now, we consider the case of single field oscillating, $\mathcal{A}_0 = 0$ and $\mathcal{B}_0 \neq 0$. Similarly, we begin with a trivial steady-state solution (nonlasing solution): $\mathcal{B}_0 = 0$, $\mathcal{M}_{B0} = 0$, $\mathcal{N}_{bb0} = \frac{\gamma_{cb}}{\gamma_b}\frac{R}{\gamma_{ct}}$, and $\mathcal{N}_{cc0} = \frac{R}{\gamma_{ct}}$. The evolution equation of the perturbations can be expressed as

$$\frac{d}{dt}\begin{pmatrix} \delta\mathcal{M}_B^*(t)+\delta\mathcal{M}_B(t) \\ \delta\mathcal{N}_{bb}(t) \\ \delta\mathcal{B}^*(t)+\delta\mathcal{B}(t) \end{pmatrix} = \mathbb{M}_B\begin{pmatrix} \delta\mathcal{M}_B^*(t)+\delta\mathcal{M}_B(t) \\ \delta\mathcal{N}_{bb}(t) \\ \delta\mathcal{B}^*(t)+\delta\mathcal{B}(t) \end{pmatrix},$$

where the characteristic matrix is given by

$$\mathbb{M}_B = \begin{pmatrix} -\Gamma_B & 0 & g_b\frac{R}{\bar{\gamma}_b} \\ 0 & -\frac{\gamma_b\gamma_{ct}}{\gamma_{ct}-\gamma_{cb}} & 0 \\ g_b & 0 & -\frac{\kappa_b}{2} \end{pmatrix}. \tag{83}$$

Following the standard linear stability analysis, we get the following cubic polynomial equation

$$s^3 + b_2 s^2 + b_1 s + b_0 = 0, \tag{84}$$

where the parameters are defined as

$$b_2 = \Gamma_B + \frac{\kappa_b}{2} + \frac{\gamma_{ct}\gamma_b}{\gamma_{ct}-\gamma_{cb}},$$
$$b_1 = \frac{\Gamma_B\kappa_b}{2} + \frac{\gamma_{ct}\gamma_b}{\gamma_{ct}-\gamma_{cb}}\left(\Gamma_B+\frac{\kappa_b}{2}\right) - \frac{Rg_b^2}{2\bar{\gamma}_b},$$
$$b_0 = \frac{\gamma_{ct}\gamma_b}{\gamma_{ct}-\gamma_{cb}}\left(\frac{\Gamma_B\kappa_b}{2} - \frac{Rg_b^2}{2\bar{\gamma}_b}\right).$$

We can further obtain the first threshold $r_{\mathrm{TH,I}}^{(b,0)}$ for the field $\mathcal{B} \neq 0$ oscillating inside the cavity, which is exactly equal to the common threshold $R_{\mathrm{TH}}^{(b,0)}$ derived in Sec. III.

One the other hand, based on the steady-state solutions of Eqs. (57)–(60) the characteristic matrix $\mathbb{M}_B$ for the single field oscillating ($\mathcal{A} = 0$ and $\mathcal{B} \neq 0$) is given by

$$\mathbb{M}_B = \begin{pmatrix} -\Gamma_B & -2g_b\mathcal{B}_0\left(1+\frac{\gamma_b}{\gamma_{ct}-\gamma_{cb}}\right) & \frac{g_b}{\mathcal{C}_b} \\ g_b\mathcal{B}_0 & -\frac{\gamma_b\gamma_{ct}}{\gamma_{ct}-\gamma_{cb}} & g_b\mathcal{M}_{B0} \\ g_b & 0 & -\frac{\kappa_b}{2} \end{pmatrix}, \tag{85}$$

and the parameters of Eq. (84) are replaced by

$$b_2 = \Gamma_B + \frac{\kappa_b}{2} + \frac{\gamma_{ct}\gamma_b}{\gamma_{ct}-\gamma_{cb}},$$
$$b_1 = \frac{\gamma_{ct}\gamma_b}{\gamma_{ct}-\gamma_{cb}}\frac{\Gamma_B\mathcal{C}_b}{\bar{\gamma}_b}\left(\bar{\gamma}_b\frac{\kappa_b^2}{4g_b^2}+R\right),$$
$$b_0 = \frac{\gamma_{ct}\gamma_b}{\gamma_{ct}-\gamma_{cb}}\frac{2g_b^2}{\bar{\gamma}_b}\left(R-\frac{\bar{\gamma}_b}{\mathcal{C}_b}\right).$$

Finally, we arrive at the second threshold

$$r_{\mathrm{TH,II}}^{(b,0)} = \frac{\bar{\gamma}_b}{\mathcal{C}_b}\frac{3+\frac{1}{\Gamma_B}\left(\frac{\kappa_b}{2}+\frac{\gamma_{ct}\gamma_b}{\gamma_{ct}-\gamma_{cb}}\right)}{1-\frac{2}{\kappa_b}\left(\Gamma_B+\frac{\gamma_{ct}\gamma_b}{\gamma_{ct}-\gamma_{cb}}\right)}. \tag{86}$$

Based on the parameters chosen in Fig. 2 the second threshold $r_{\mathrm{TH,II}}^{(b,0)}$ does not exist in the good-cavity limit. Actually, the bad-cavity condition is usually regarded as a necessary condition for laser instability to occur.

3. $\mathcal{A}_0 \neq 0$ and $\mathcal{B}_0 \neq 0$

For the single field oscillating inside the cavity, the first threshold $r_{\mathrm{TH,I}}^{(a,0)}$ ($r_{\mathrm{TH,I}}^{(b,0)}$) is exactly equal to the common laser threshold $R_{\mathrm{TH}}^{(a,0)}$ ($R_{\mathrm{TH}}^{(b,0)}$). Now we consider the stability of the steady-state solution in the case of both fields oscillating. First, we assume that field $\mathcal{A}_0$ is already oscillating inside the cavity and field $\mathcal{B}_0 = 0$. In this case, the linear stability analysis leads the following dynamic equation

$$\frac{d}{dt}\mathbb{L} = \mathbb{M}_{AB} \times \mathbb{L}, \tag{87}$$

where the column matrix $\mathbb{L}$ and characteristic matrix $\mathbb{M}$ are expressed as

$$\mathbb{L} = (\delta\mathcal{M}_A^*(t) + \delta\mathcal{M}_A(t)\ \delta\mathcal{M}_B^*(t) + \delta\mathcal{M}_B(t)\ \delta\mathcal{M}_C^*(t) + \delta\mathcal{M}_C(t)\ \delta\mathcal{N}_{aa}(t)\ \delta\mathcal{N}_{bb}(t)\ \delta\mathcal{A}^*(t) + \delta\mathcal{A}(t)\ \delta\mathcal{B}^*(t) + \delta\mathcal{B}(t))^T,$$

$$\mathbb{M}_{AB} = \begin{pmatrix} -\Gamma_A & 0 & 0 & -2g_a\mathcal{A}_0\left(1+\frac{\gamma_a}{\gamma_c'}\right) & -2g_a\mathcal{A}_0\frac{\gamma_b}{\gamma_c'} & g_a\left(\mathcal{N}_{cc0}^{(a,0)} - \mathcal{N}_{aa0}^{(a,0)}\right) & 0 \\ 0 & -\Gamma_B & -g_a\mathcal{A}_0 & 0 & 0 & 0 & g_b\left(\mathcal{N}_{cc0}^{(a,0)} - \mathcal{N}_{bb0}^{(a,0)}\right) \\ 0 & g_a\mathcal{A}_0 & -\Gamma_C & 0 & 0 & 0 & g_b\mathcal{M}_{A0} \\ g_a\mathcal{A}_0 & 0 & 0 & -\gamma_a\left(1+\frac{\gamma_{ca}}{\gamma_c'}\right) & -\gamma_b\frac{\gamma_{ca}}{\gamma_c'} & g_a\mathcal{M}_{A0} & 0 \\ 0 & 0 & 0 & -\gamma_a\frac{\gamma_{cb}}{\gamma_c'} & -\gamma_b\left(1+\frac{\gamma_{cb}}{\gamma_c'}\right) & 0 & 0 \\ g_a & 0 & 0 & 0 & 0 & -\frac{\kappa_a}{2} & 0 \\ 0 & g_b & 0 & 0 & 0 & 0 & -\frac{\kappa_b}{2} \end{pmatrix},$$

where $\mathcal{A}_0^2 = \mathcal{I}_{a0}^{(a,0)}$ and $\mathcal{M}_{A0} = \frac{\kappa_a}{2g_a}\mathcal{A}_0$. From matrix $\mathbb{M}_{AB}$, one can obtain a characteristic equation of the seventh order

$$s^7 + c_6 s^6 + c_5 s^5 + c_4 s^4 + c_3 s^3 + c_2 s^2 + c_1 s + c_0 = 0. \tag{88}$$

Parameters c_i $(i = 1, \ldots, 6)$ are very complicated and for simplicity we do not list their expressions here. Again, substituting $s = i\Omega$ into Eq. (88) and canceling the Ω term, we arrive at $c_0 = 0$ and obtain a critical pump value $r_{\mathrm{TH,I}}^{(a,1)}$, which is exactly equal to $R_{\mathrm{TH}}^{(a,1)}$. When the pump rate exceeds the first threshold $r_{\mathrm{TH,I}}^{(b,1)}$, both fields $\mathcal{A}_0$ and $\mathcal{B}_0$ can oscillate inside the cavity.

Second, we assume that field $\mathcal{B}_0 \neq 0$ is already oscillating inside the cavity and field $\mathcal{A}_0 = 0$. In this case, the characteristic matrix can be expressed as

$$\mathbb{M}_{AB} = \begin{pmatrix} -\Gamma_A & 0 & -g_b\mathcal{B}_0 & 0 & 0 & g_a\left(\mathcal{N}_{cc0}^{(b,0)} - \mathcal{N}_{aa0}^{(b,0)}\right) & 0 \\ 0 & -\Gamma_B & 0 & -2g_b\mathcal{B}_0\frac{\gamma_a}{\gamma_c'} & -2g_b\mathcal{B}_0\left(1+\frac{\gamma_b}{\gamma_c'}\right) & 0 & g_b\left(\mathcal{N}_{cc0}^{(b,0)} - \mathcal{N}_{bb0}^{(b,0)}\right) \\ g_b\mathcal{B}_0 & 0 & -\Gamma_C & 0 & 0 & g_a\mathcal{M}_{B0} & 0 \\ 0 & 0 & 0 & -\gamma_a\left(1+\frac{\gamma_{ca}}{\gamma_c'}\right) & -\gamma_b\frac{\gamma_{ca}}{\gamma_c'} & 0 & 0 \\ 0 & g_b\mathcal{B}_0 & 0 & -\gamma_a\frac{\gamma_{cb}}{\gamma_c'} & -\gamma_b\left(1+\frac{\gamma_{cb}}{\gamma_c'}\right) & 0 & g_b\mathcal{M}_{B0} \\ g_a & 0 & 0 & 0 & 0 & -\frac{\kappa_a}{2} & 0 \\ 0 & g_b & 0 & 0 & 0 & 0 & -\frac{\kappa_b}{2} \end{pmatrix}, \tag{89}$$

where $\mathcal{B}_0^2 = \mathcal{I}_{b0}^{(b,0)}$ and $\mathcal{M}_{B0} = \frac{\kappa_b}{2g_b}\mathcal{B}_0$. Then, based on Eq. (89), we derive the characteristic equation, substitute $s = i\Omega$, and obtain another first threshold $r_{\mathrm{TH,I}}^{(b,1)}$ for both fields oscillating, which is exactly equal to $R_{\mathrm{TH}}^{(b,1)}$. For deriving the second threshold for both fields oscillating, we have the following characteristic matrix

$$\mathbb{M}_{AB} = \begin{pmatrix} -\Gamma_A & 0 & -g_b\mathcal{B}_0 & -2g_a\mathcal{A}_0\left(1+\frac{\gamma_a}{\gamma_c'}\right) & -2g_a\mathcal{A}_0\frac{\gamma_b}{\gamma_c'} & g_a\left(\mathcal{N}_{cc0}^{(1)} - \mathcal{N}_{aa0}^{(1)}\right) & -g_b\mathcal{M}_{C0} \\ 0 & -\Gamma_B & -g_a\mathcal{A}_0 & -2g_b\mathcal{B}_0\frac{\gamma_a}{\gamma_c'} & -2g_b\mathcal{B}_0\left(1+\frac{\gamma_b}{\gamma_c'}\right) & -g_a\mathcal{M}_{C0} & g_b\left(\mathcal{N}_{cc0}^{(1)} - \mathcal{N}_{bb0}^{(1)}\right) \\ g_b\mathcal{B}_0 & g_a\mathcal{A}_0 & -\Gamma_C & 0 & 0 & g_a\mathcal{M}_{B0} & g_b\mathcal{M}_{A0} \\ g_a\mathcal{A}_0 & 0 & 0 & -\gamma_a\left(1+\frac{\gamma_{ca}}{\gamma_c'}\right) & -\gamma_b\frac{\gamma_{ca}}{\gamma_c'} & g_a\mathcal{M}_{A0} & 0 \\ 0 & g_b\mathcal{B}_0 & 0 & -\gamma_a\frac{\gamma_{cb}}{\gamma_c'} & -\gamma_b\left(1+\frac{\gamma_{cb}}{\gamma_c'}\right) & 0 & g_b\mathcal{M}_{B0} \\ g_a & 0 & 0 & 0 & 0 & -\frac{\kappa_a}{2} & 0 \\ 0 & g_b & 0 & 0 & 0 & 0 & -\frac{\kappa_b}{2} \end{pmatrix},$$

which can be derived based on the steady-state solutions (62)–(66). Again, we solve the equation

$$\det|s - \mathbb{M}_{AB}| = 0. \tag{90}$$

An unstable steady-state solution requires that any solution of Eq. (90) has a positive real part. Based on this condition, one can judge the stability of a steady-state solution. For the parameters chosen in Fig. 2 all the steady-state solutions are stable. As we have said, the bad-cavity condition is a necessary condition for laser instability to occur.

B. Quantum phase noise and laser linewidth

Above, we considered the stability of the steady-state solutions obtain in Sec. III. Now, we investigate the influence of fluctuations on the field phases and laser linewidths.

We take the Fourier transform of all variables and convert the differential equations in the time domain into algebraic equations in the frequency domain, for example,

$$\delta\mathcal{N}_{aa}(\omega) = \frac{1}{\sqrt{2\pi}} \int_{-\infty}^{+\infty} dt\, \delta\mathcal{N}_{aa}(t) e^{i\omega t}. \tag{91}$$

In order not to overcharge the notation, we adopt the same symbol for both members of a Fourier-transform pair, which will therefore be distinguished through the time or frequency argument. Here, for simplicity, we do not list the linear equations for the Fourier amplitudes. The Fourier-transformed fluctuation forces satisfy the equation

$$\langle \mathcal{F}_\alpha(\omega)\mathcal{F}_\beta(\omega')\rangle = \mathcal{D}_{\alpha\beta}\delta(\omega+\omega'). \tag{92}$$

The solution of this linear system is straightforward. The field phase quadrature components of two laser fields are defined as

$$\delta Y_A(\omega) = \frac{1}{2i}[\delta\mathcal{A}(\omega) - \delta\mathcal{A}^*(-\omega)], \tag{93}$$

$$\delta Y_B(\omega) = \frac{1}{2i}[\delta\mathcal{B}(\omega) - \delta\mathcal{B}^*(-\omega)], \tag{94}$$

which are proportional to the phase fluctuations of two fields, $\delta Y_A \propto \delta\phi_a$ and $\delta Y_B \propto \delta\phi_b$, respectively. For the laser system working well above threshold, the diffusion coefficient of the field phase fluctuation gives the laser linewidth. Next, we discuss the linewidths of two laser fields in different oscillating cases.

1. $\mathcal{A}_0 \neq 0$ and $\mathcal{B}_0 = 0$

In this case, the phase quadrature component of field $\mathcal{A}_0$ can be expressed as the following simple form:

$$\delta Y_A^{(a,0)}(\omega) = \frac{g_a[\mathcal{F}_A(\omega) - \mathcal{F}_A^*(-\omega)] + \tilde{\Gamma}_A[\mathcal{F}_{\kappa a}(\omega) - \mathcal{F}_{\kappa a}^*(-\omega)]}{2i[(\kappa_a/2 - i\omega)\tilde{\Gamma}_A - g_a^2(\mathcal{N}_{cc0} - \mathcal{N}_{aa0})]}, \tag{95}$$

where $\tilde{\Gamma}_A \equiv \Gamma_A - i\omega$. One can see that the field phase fluctuation only comes from the noises of atomic polarization $\mathcal{F}_A(t)$ and cavity $\mathcal{F}_{\kappa a}(t)$.

The autocorrelation function of the phase quadrature is δ function correlated,

$$\langle \delta Y_A^{(a,0)}(\omega)\delta Y_A^{(a,0)}(\omega')\rangle = \left(\delta Y_{A,0}^2\right)_\omega \delta(\omega+\omega'). \tag{96}$$

For a small fluctuation of the field phase, the spectrum of the phase fluctuation is simply related to the spectrum of the phase quadrature component of the field fluctuation, namely, $(\delta\phi_{a,0}^2)_\omega = (\delta Y_{A,0}^2)_\omega / \mathcal{I}_{a0}^{(a,0)}$. $(\delta\phi_{a,0}^2)_\omega$ and $(\delta Y_{A,0}^2)_\omega$ correspond to the case of $\mathcal{A}_0 \neq 0$ and $\mathcal{B}_0 = 0$. Figure 3 displays $(\delta\phi_{a,0}^2)_\omega$ as a function of frequency ω. One can see that for $\omega < (\Gamma_A + \kappa_a/2)$ the spectrum $(\delta\phi_{a,0}^2)_\omega$ scales as ω^{-2}, i.e., the character of white frequency noise. However, $(\delta\phi_{a,0}^2)_\omega$ is proportional to ω^{-4} for $\omega > (\Gamma_A + \kappa_a/2)$, which originates from the atomic memory effect associated with the transient behavior of the atomic polarization. For a measurement with a time scale much shorter than $(\Gamma_A + \kappa_a/2)^{-1}$, the spontaneous-emission events are correlated and this leads to the reduction of the phase noise [30,31].

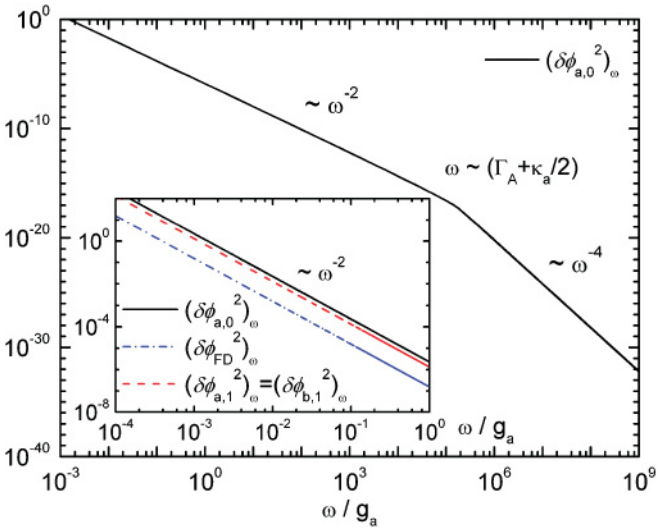

FIG. 3. (Color online) Spectrum of the field phase fluctuation. In the case of $\mathcal{A}_0 \neq 0$ and $\mathcal{B}_0 = 0$, spectrum $(\delta\phi_{a,0}^2)_\omega$ is proportional to ω^{-2} for $\omega < (\Gamma_A + \kappa_a/2)$ while $(\delta\phi_{a,0}^2)_\omega$ scales as ω^{-4} for $\omega > (\Gamma_A + \kappa_a/2)$ due to the atomic memory effect. The inset illustrates the phase noise spectra of the laser fields $\mathcal{A}_0 \neq 0$ and $\mathcal{B}_0 \neq 0$, and the frequency-difference field for $g_a = g_b$. The pumping rate is chosen to be $R/R_{\rm TH}^{(a,0)} = 10^3$ and all the other parameters are the same as in Fig. 2. The phase spectrum is given in units of g_a^{-1}.

One can directly calculate the correlation function of the time derivative of the field phase fluctuation:

$$\left\langle \delta\dot{\phi}_a^{(a,0)}(t)\delta\dot{\phi}_a^{(a,0)}(t')\right\rangle = \frac{1}{2\pi}\int_{-\infty}^{+\infty} d\omega e^{-i\omega(t-t')}\omega^2\left(\delta\phi_{a,0}^2\right)_\omega. \tag{97}$$

When $|t-t'|$ is much shorter than all the other characteristic times of the laser system, this expression becomes

$$\left\langle \delta\dot{\phi}_a^{(a,0)}(t)\delta\dot{\phi}_a^{(a,0)}(t')\right\rangle = D^{(a,0)}\delta(t-t'), \tag{98}$$

which corresponds to a Markovian times evolution for the field phase, and $D^{(a,0)}$ gives the linewidth of laser field $\mathcal{A}_0$ with $\mathcal{B}_0$ [32]. From Eq. (95), we obtain

$$D^{(a,0)} = D_{\rm ST}^{(a,0)} + D_\kappa^{(a,0)}, \tag{99}$$

where the first term on the right side

$$D_{\rm ST}^{(a,0)} = \left(\frac{\Gamma_A}{\Gamma_A + \kappa_a/2}\right)^2 \frac{g_a^2 \mathcal{N}_{cc0}^{(a,0)}}{\Gamma_A \mathcal{I}_{a0}^{(a,0)}} \tag{100}$$

is from the noise of atomic polarization $\mathcal{F}_A(t)$ and

$$D_\kappa^{(a,0)} = \left(\frac{\Gamma_A}{\Gamma_A + \kappa_a/2}\right)^2 \frac{\kappa_a}{4\mathcal{I}_{a0}^{(a,0)}}(2n_{\rm th}+1) \tag{101}$$

comes from the thermal noise of cavity $\mathcal{F}_{\kappa a}(t)$.

$D_{\rm ST}^{(a,0)}$ is the quantum-limited laser linewidth, which is also called the intrinsic or natural linewidth. If the atomic polarization decay rate is much faster than the cavity loss rate, i.e., the good-cavity limit $\Gamma_A \gg \kappa_a$, we are left with the usual ST diffusion coefficient. In contrast, in the bad-cavity limit $\Gamma_A \ll \kappa_a$, $D_{\rm ST}^{(a,0)}$ can well exceed the ST limit. The constant 1 in the expression of $D_\kappa^{(a,0)}$ is due to the contribution of vacuum

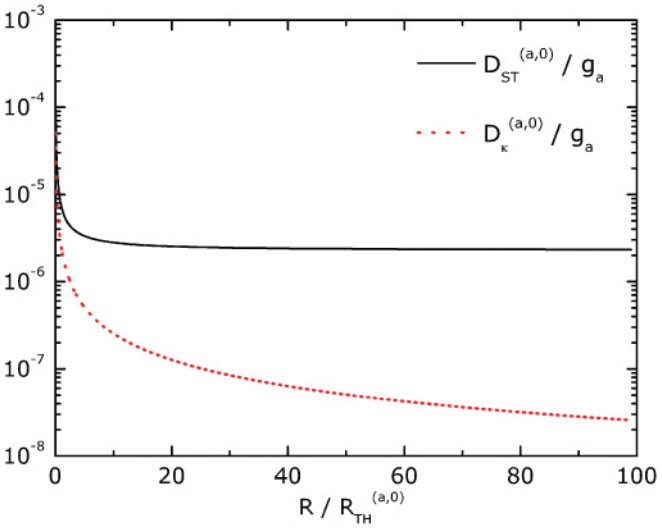

FIG. 4. (Color online) Dependence of linewidths $D_{\rm ST}^{(a,0)}$ and $D_{\kappa}^{(a,0)}$ on the pumping rate R for $g_b = 0$ ($\mathcal{A}_0 \neq 0$ and $\mathcal{B}_0 = 0$). All the other parameters are the same as in Fig. 2.

fluctuations. There are two ways to reduce the influence of cavity thermal noise on laser linewidth: (i) Decrease the temperature of the cavity down to absolute zero, which is difficult to implement in experiment. (ii) In the bad-cavity limit, $\Gamma_A \ll \kappa_a$, $D_{\kappa}^{(a,0)}$ is approximately inversely proportional to κ_a, and enlarging the cavity loss rate κ_a can reduce $D_{\kappa}^{(a,0)}$. Both $D_{\rm ST}^{(a,0)}$ and $D_{\kappa}^{(a,0)}$ are inversely proportional to the photon number $\mathcal{I}_{a0}^{(a,0)}$ inside the cavity.

Figure 4 displays these two linewidths as a function of pumping rate R. Increasing the photon number can always reduce the influence of cavity thermal noise on laser linewidth, but $D_{\rm ST}^{(a,0)}$ is saturated for a high pumping rate since the population of the upper lasing level $\mathcal{N}_{cc0}^{(a,0)}$ is also increased. It denotes that the efficiency of atoms on level $|c\rangle$ to produce the coherent photons is saturated. Additionally, from Eq. (100) one can see that decreasing the atom-cavity coupling strength g_a can well reduce the linewidth $D_{\rm ST}^{(a,0)}$, but the threshold of pumping rate $R_{\rm TH}^{(a,0)}$ significantly increases.

2. $\mathcal{A}_0 = 0$ and $\mathcal{B}_0 \neq 0$

Similarly, we can derive the phase quadrature component of field $\mathcal{B}_0 \neq 0$ in the case of $\mathcal{A}_0 = 0$,

$$\delta Y_B^{(b,0)}(\omega) = \frac{g_b[\mathcal{F}_B(\omega) - \mathcal{F}_B^*(-\omega)] + \tilde{\Gamma}_B[\mathcal{F}_{\kappa b}(\omega) - \mathcal{F}_{\kappa b}^*(-\omega)]}{2i\left[(\kappa_b/2 - i\omega)\tilde{\Gamma}_B - g_b^2(\mathcal{N}_{cc0} - \mathcal{N}_{bb0})\right]}, \tag{102}$$

where $\tilde{\Gamma}_B \equiv \Gamma_B - i\omega$. Based on Eq. (102), one can obtain the laser linewidth of field $\mathcal{B}_0$ as

$$D^{(b,0)} = D_{\rm ST}^{(b,0)} + D_{\kappa}^{(b,0)}, \tag{103}$$

where

$$D_{\rm ST}^{(b,0)} = \left(\frac{\Gamma_B}{\Gamma_B + \kappa_b/2}\right)^2 \frac{g_b^2 \mathcal{N}_{cc0}^{(b,0)}}{\Gamma_B \mathcal{I}_{b0}^{(b,0)}} \tag{104}$$

is from the noise of atomic polarization $\mathcal{F}_B(t)$ and

$$D_{\kappa}^{(b,0)} = \left(\frac{\Gamma_B}{\Gamma_B + \kappa_b/2}\right)^2 \frac{\kappa_b}{4\mathcal{I}_{b0}^{(b,0)}}(2n_{\rm th} + 1) \tag{105}$$

comes from the thermal noise of cavity $\mathcal{F}_{\kappa b}(t)$.

3. $\mathcal{A}_0 \neq 0$ and $\mathcal{B}_0 \neq 0$

The expression of phase quadratures of two fields in this case are very complicated. Here we do not list their expressions. In Fig. 3, we show the spectrums of field phase noises $(\delta\phi_{a,1}^2)_\omega$ and $(\delta\phi_{b,1}^2)_\omega$ in the lower frequency region. $(\delta\phi_{a,1}^2)_\omega$ and $(\delta\phi_{b,1}^2)_\omega$ correspond to the case of $\mathcal{A}_0 \neq 0$ and $\mathcal{B}_0 \neq 0$. Same as $(\delta\phi_{a,0}^2)_\omega$, both $(\delta\phi_{a,1}^2)_\omega$ and $(\delta\phi_{b,1}^2)_\omega$ scale as ω^{-2}, which denotes that the white frequency noise dominates the field phase fluctuations in the lower frequency region. In this case, we obtain the laser linewidths $D^{(a,1)}$ and $D^{(b,1)}$ of fields $\mathcal{A}_0$ and $\mathcal{B}_0$,

$$D^{(a,1)} = D_{\rm ST}^{(a,1)} + D_{\kappa}^{(a,1)}, \tag{106}$$
$$D^{(b,1)} = D_{\rm ST}^{(b,1)} + D_{\kappa}^{(b,1)}, \tag{107}$$

where the linewidths induced by the noises of atomic polarizations $\mathcal{F}_A(t)$, $\mathcal{F}_B(t)$, and $\mathcal{F}_C(t)$ can be expressed as

$$D_{\rm ST}^{(a,1)} = \frac{-1}{4\mathcal{I}_{a0}^{(1)}(\mathcal{K}_1\mathcal{K}_2 - \mathcal{K}_3\mathcal{K}_4)^2} \times \left[\mathcal{K}_3 g_b\left(\Gamma_C\mathcal{L}_B + g_a\sqrt{\mathcal{I}_{a0}^{(1)}}\mathcal{L}_C\right) + \mathcal{K}_2 g_a\left(\Gamma_C\mathcal{L}_A - g_b\sqrt{\mathcal{I}_{b0}^{(1)}}\mathcal{L}_C\right)\right]^2, \tag{108}$$

$$D_{\rm ST}^{(b,1)} = \frac{-1}{4\mathcal{I}_{b0}^{(1)}(\mathcal{K}_1\mathcal{K}_2 - \mathcal{K}_3\mathcal{K}_4)^2} \times \left[\mathcal{K}_1 g_b\left(\Gamma_C\mathcal{L}_B + g_a\sqrt{\mathcal{I}_{a0}^{(1)}}\mathcal{L}_C\right) + \mathcal{K}_4 g_a\left(\Gamma_C\mathcal{L}_A - g_b\sqrt{\mathcal{I}_{b0}^{(1)}}\mathcal{L}_C\right)\right]^2, \tag{109}$$

and the linewidths caused by the thermal noise of cavities are given by

$$D_{\kappa}^{(a,1)} = \frac{(2n_{\rm th} + 1)}{4\mathcal{I}_{a0}^{(1)}(\mathcal{K}_1\mathcal{K}_2 - \mathcal{K}_3\mathcal{K}_4)^2} \times \left[\left(\mathcal{K}_2\Sigma_a - \mathcal{K}_3 g_b^2\mathcal{I}_{\rm av}\right)^2\kappa_a + \left(\mathcal{K}_3\Sigma_b - \mathcal{K}_2 g_a^2\mathcal{I}_{\rm av}\right)^2\kappa_b\right], \tag{110}$$

$$D_{\kappa}^{(b,1)} = \frac{(2n_{\rm th} + 1)}{4\mathcal{I}_{b0}^{(1)}(\mathcal{K}_1\mathcal{K}_2 - \mathcal{K}_3\mathcal{K}_4)^2} \times \left[\left(\mathcal{K}_4\Sigma_a - \mathcal{K}_1 g_b^2\mathcal{I}_{\rm av}\right)^2\kappa_a + \left(\mathcal{K}_1\Sigma_b - \mathcal{K}_4 g_a^2\mathcal{I}_{\rm av}\right)^2\kappa_b\right]. \tag{111}$$

In above equations we have defined $\Sigma_a = \Gamma_C\Gamma_A + g_b^2\mathcal{I}_{b0}^{(1)}$, $\Sigma_b = \Gamma_C\Gamma_B + g_a^2\mathcal{I}_{a0}^{(1)}$, $\mathcal{K}_1 = \Sigma_a + \frac{\kappa_a}{2}\Gamma_C - g_a g_b\mathcal{I}_{b0}^{(1)}\mathcal{Q}$, $\mathcal{K}_2 = \Sigma_b + \frac{\kappa_b}{2}\Gamma_C - g_a g_b\mathcal{I}_{a0}^{(1)}\mathcal{Q}$, $\mathcal{K}_3 = g_a\mathcal{I}_{\rm av}(g_a - g_b\mathcal{Q})$, $\mathcal{K}_4 = g_b\mathcal{I}_{\rm av}(g_b - g_a\mathcal{Q})$, $\mathcal{I}_{\rm av} = \sqrt{\mathcal{I}_{a0}^{(1)}\mathcal{I}_{b0}^{(1)}}$, and a symbolic operation

$$\mathcal{L}_\alpha\mathcal{L}_\beta \equiv \mathcal{D}(\mathcal{M}_\alpha^*, \mathcal{M}_\beta^*) + \mathcal{D}(\mathcal{M}_\beta, \mathcal{M}_\alpha) - \mathcal{D}(\mathcal{M}_\alpha^*, \mathcal{M}_\beta) - \mathcal{D}(\mathcal{M}_\beta^*, \mathcal{M}_\alpha). \tag{112}$$

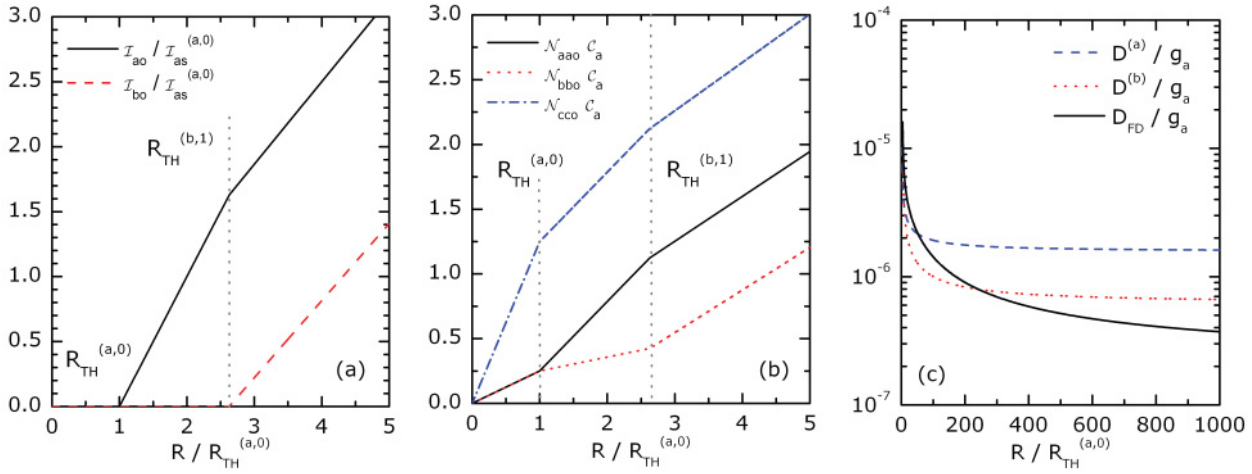

FIG. 5. (Color online) Dependence of photon numbers inside the cavity $\mathcal{I}_{a0}$ and $\mathcal{I}_{b0}$, the atomic populations of levels $|a,b,c\rangle$, and linewidths $D^{(a)}$, $D^{(b)}$, and $D_{\rm FD}$ on the pumping rate R. For all curves, $g_b/g_a = 0.8$ and all the other parameters are the same as in Fig. 2.

Equation (112) ensures that $D_{\rm ST}^{(a,1)} > 0$ and $D_{\rm ST}^{(b,1)} > 0$. Figure 3 shows that $(\delta\phi_{a,1}^2)_\omega$ ($g_a = g_b$) is very close to $(\delta\phi_{a,0}^2)_\omega$ ($g_b = 0$), which denotes that the oscillation of field $\mathcal{B}_0$ does not strongly affect the phase fluctuation of field $\mathcal{A}_0$.

Figure 5(a) displays the photon numbers inside the cavity, $\mathcal{I}_{a0}$ and $\mathcal{I}_{b0}$, as a function of the pumping rate R. When field $\mathcal{B}_0$ starts to oscillate, the dependence of laser field $\mathcal{A}_0$ on the pumping rate changes and an inflection point is presented, which can be also clearly found in the dependence of atomic populations on R, as shown in Fig. 5(b). Laser linewidths of two fields $D^{(a)}$ and $D^{(b)}$ are shown in Fig. 5(c). Before field $\mathcal{B}_0$ oscillating, $D^{(a)}$ decreases with R being increased since $D^{(a)}$ is inversely proportional to the photon number $\mathcal{I}_{a0}^{(a,0)}$. When field $\mathcal{B}_0$ starts to oscillate, laser linewidth $D^{(b)}$ strongly decreases and can be smaller than $D^{(a)}$ since the coupling strength g_b is smaller than g_a. Both linewidths $D^{(a)}$ and $D^{(b)}$ are saturated for a high pumping rate.

4. *Phase-matching effect in Λ-type laser system*

Above we discussed the laser linewidths in different oscillating cases. Now we consider the coherence between two laser fields. For this we define a function to describe the frequency-difference (FD) field of two lasers, $\mathcal{W}(t) = \mathcal{A}(t)\mathcal{B}^*(t)/\mathcal{I}_{\rm av}$, whose fluctuation around the steady state can be expressed as

$$\delta\mathcal{W}(\omega) = \frac{\delta\mathcal{A}(\omega)}{\sqrt{\mathcal{I}_{a0}^{(1)}}} + \frac{\delta\mathcal{B}^*(-\omega)}{\sqrt{\mathcal{I}_{b0}^{(1)}}} \tag{113}$$

in the frequency domain. The phase quadrature of the FD field is given by

$$\delta Y_W(\omega) = \frac{1}{2i}[\delta\mathcal{W}(\omega) - \delta\mathcal{W}^*(-\omega)], \tag{114}$$

based on which one can derive the spectrum of phase noise of the FD field $(\delta\phi_{\rm FD}^2)_\omega$. In Fig. 3, we compare the spectrums $(\delta\phi_{a,1}^2)_\omega$, $(\delta\phi_{b,1}^2)_\omega$, and $(\delta\phi_{\rm FD}^2)_\omega$ in the lower frequency region and find that $(\delta\phi_{\rm FD}^2)_\omega$ can be much smaller than either laser field.The linewidth of the FD field can be expressed as

$$\begin{aligned} D_{\rm FD} = {} & D_{\rm ST}^{(a,1)} + D_{\rm ST}^{(b,1)} + \frac{1}{2\mathcal{I}_{\rm av}(\mathcal{K}_1\mathcal{K}_2 - \mathcal{K}_3\mathcal{K}_4)^2} \\ & \times \left[\mathcal{K}_3 g_b\left(\Gamma_C\mathcal{L}_B + g_a\sqrt{\mathcal{I}_{a0}^{(1)}}\mathcal{L}_C\right)\right. \\ & \left. + \mathcal{K}_2 g_a(\Gamma_C\mathcal{L}_A - g_b\sqrt{\mathcal{I}_{b0}^{(1)}}\mathcal{L}_C)\right] \\ & \times \left[\mathcal{K}_1 g_b\left(\Gamma_C\mathcal{L}_B + g_a\sqrt{\mathcal{I}_{a0}^{(1)}}\mathcal{L}_C\right)\right. \\ & \left. + \mathcal{K}_4 g_a\left(\Gamma_C\mathcal{L}_A - g_b\sqrt{\mathcal{I}_{b0}^{(1)}}\mathcal{L}_C\right)\right] \\ & - \frac{(2n_{\rm th}+1)}{2\mathcal{I}_{\rm av}(\mathcal{K}_1\mathcal{K}_2 - \mathcal{K}_3\mathcal{K}_4)^2}\left[\left(\mathcal{K}_2\Sigma_a - \mathcal{K}_3 g_b^2\mathcal{I}_{\rm av}\right)\right. \\ & \times \left.\left(\mathcal{K}_4\Sigma_a - \mathcal{K}_1 g_b^2\mathcal{I}_{\rm av}\right)\kappa_a + \left(\mathcal{K}_3\Sigma_b - \mathcal{K}_2 g_a^2\mathcal{I}_{\rm av}\right)\right. \\ & \left. \times \left(\mathcal{K}_1\Sigma_b - \mathcal{K}_4 g_a^2\mathcal{I}_{\rm av}\right)\kappa_b\right]. \end{aligned}$$

$D_{\rm FD}$ denotes the quantum-limited coherence between two laser fields, which is composed of the intrinsic linewidths of two lasers and their interference terms.

In Fig. 5(c), we show the linewidth $D_{\rm FD}$ can be much smaller than either $D^{(a)}$ or $D^{(b)}$, which denotes that the coherence between two laser fields well exceeds their intrinsic coherences. In this case, although each laser field has a large phase fluctuation, their relative phase fluctuation can be small, which is to say two field phases match each other. Larger field intensities lead to smaller linewidth $D_{\rm FD}$, which is different from the phase-matching effect based on stimulated absorption (the final coherence in this case is limited by saturated broadening [17]). Additionally, $D_{\rm FD}$ can well exceed the natural damping rate Γ_C between two lower states $|a,b\rangle$.

Figure 6 displays the photon numbers and linewidths changing with the coupling strength g_b for a fixed pumping rate. We can see that in the region of two fields oscillating, $\mathcal{I}_{a0}$ and $\mathcal{I}_{b0}$ are quite different with each other. For smaller coupling strength g_a (g_b), photon number $\mathcal{I}_{a0}$ ($\mathcal{I}_{b0}$) is smaller but linewidth $D^{(a)}$ ($D^{(b)}$) is also smaller due to $D^{(a)} \propto \mathcal{I}_{a0}^{-1}$,

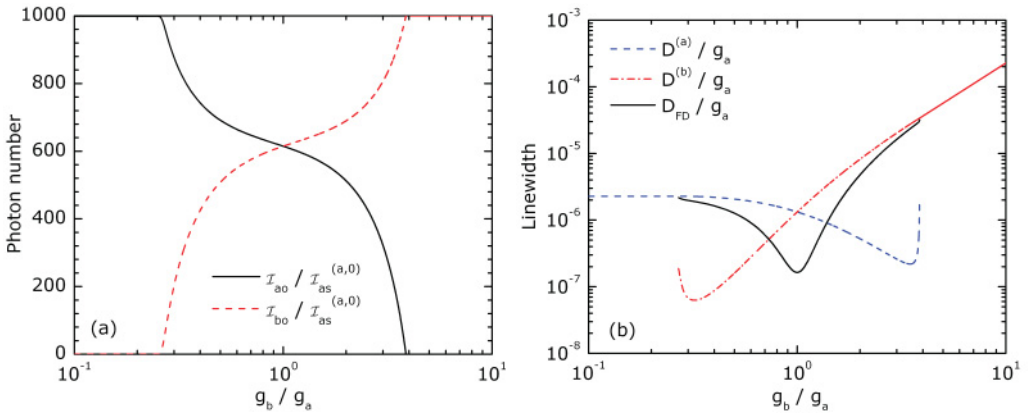

FIG. 6. (Color online) Photon numbers I_{a0} and I_{b0} and linewidths $D^{(a)}$, $D^{(b)}$, and $D_{\rm FD}$ as a function of the coupling strength g_b for a pumping rate $R/R_{\rm TH}^{(a,0)} = 10^3$. All the other parameters are the same as in Fig. 5.

$D^{(b)} \propto \mathcal{I}_{b0}^{-1}$, $D^{(a)} \propto g_a^2$, and $D^{(b)} \propto g_b^2$. Additionally, linewidth $D_{\rm FD}$ can be much smaller than either of the laser linewidths, and one can get the minimum linewidth $D_{\rm FD}$ of the FD field for $g_a = g_b$.

Figure 7 shows the linewidths of two laser fields and the FD field as a function of cavity loss rates from the good-cavity limit to the edge of the bad-cavity limit in the case of maximum coherence of the FD field. Compared with the case of a single field oscillating, linewidths $D^{(a,1)}$ and $D^{(b,1)}$ are quite close to $D^{(a,0)}$, which denotes that one field oscillating does not strongly affect the coherence of the other laser field. Meanwhile, the coherence of the FD field can well exceed that of either laser field in the whole good-cavity region. However, based on the linear stability analysis, we find that

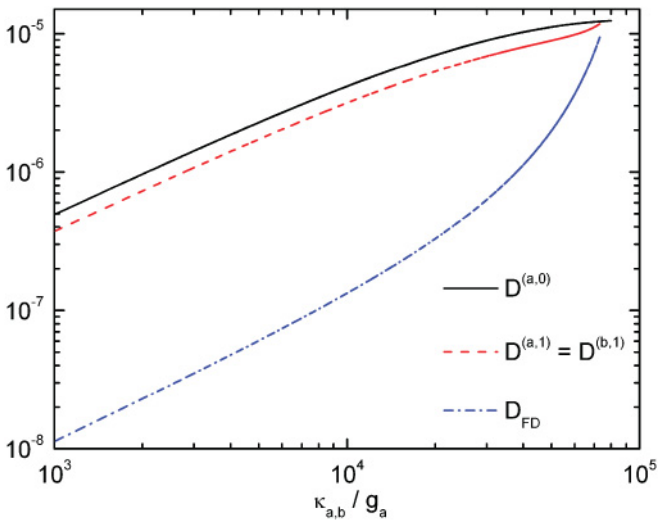

FIG. 7. (Color online) Field linewidths as a function of cavity loss rate $\kappa_a = \kappa_b$. The solid line denotes the single laser oscillating inside the cavity with $g_b = 0$ while the dash and dash-dot lines correspond to the case of two fields oscillating with $g_a = g_b$. For all curves $\Gamma_C/g_a = 10^5$ and $R/R_{\rm TH}^{(a,0)} = 10^3$. All the other parameters are the same as in Fig. 5. The linear stability analysis has already been considered. For a high pump rate $R/R_{\rm TH}^{(a,0)} = 10^3$, the stable steady-state solution does not exist any more in the bad-cavity region.

there is no stable field oscillation in the bad-cavity region for a high pump rate. Therefore, the instability of the steady state can substantially restrict the region of the phase-matching effect.

We should note that the principle of the phase-matching effect discussed here is different from that in Ref. [17]. In Ref. [17], the effect occurs because of the nonadiabatic atom-field interaction, which requires that the coherence between two lower atomic levels is much higher than the coherence of either laser fields, i.e., Γ_C should be much smaller than either laser linewidths. Actually, atoms work as a filter, which suppresses the phase fluctuation of the FD field. However, here the phase-matching effect happens because two laser fields have the same upper lasing level and each atom simultaneously contributes coherent photons to either field via the simulated emission, for which Γ_C can be much larger than $D^{(a,b)}$.

V. EXAMPLE: Nd:YAG LASER

Here we take a Nd:YAG (chemical formula Nd:$Y_3Al_5O_{12}$) laser, which is a typical four-level system and homogeneous broadening, as an example to show this quantum-limited phase-matching effect. Figure 8 displays the level scheme of the Nd:YAG system. The population inversion is achieved by exciting the Nd^{3+} ions by optical pumping into the $[^4F_{5/2}, ^2H_{9/2}]$ pump bands, from which they decay nonradiatively into the metastable upper laser state $^4F_{3/2}$ that has a fluorescence lifetime of $\tau(^4F_{3/2}) = 230\ \mu$s. The branching ratio of emission from $^4F_{3/2}$ is as follows [33]: $^4F_{3/2} \rightarrow {}^4I_{9/2} = 0.25$, $^4F_{3/2} \rightarrow {}^4I_{11/2} = 0.60$, $^4F_{3/2} \rightarrow {}^4I_{13/2} = 0.14$, and $^4F_{3/2} \rightarrow {}^4I_{15/2} < 0.01$. At room temperature only $f_{R_2} = 40\%$ of the $^4F_{3/2}$ population is at level R_2, while the remaining $f_{R_1} = 60\%$ are at the lower sublevel R_1 according to Boltzmann's law.

There are two common laser transitions with wavelengths of 1319 and 1064 nm originating from the R_2 component of the $^4F_{3/2}$ state and terminating at the X_1 and Y_3 components of the $^4I_{13/2}$ and $^4I_{11/2}$ levels, respectively. Atoms on $^4I_{13/2}$ and $^4I_{11/2}$ levels can quickly return back to the ground $^4I_{9/2}$ level via the nonradiative transition. However, for the Nd:YAG ceramic, it

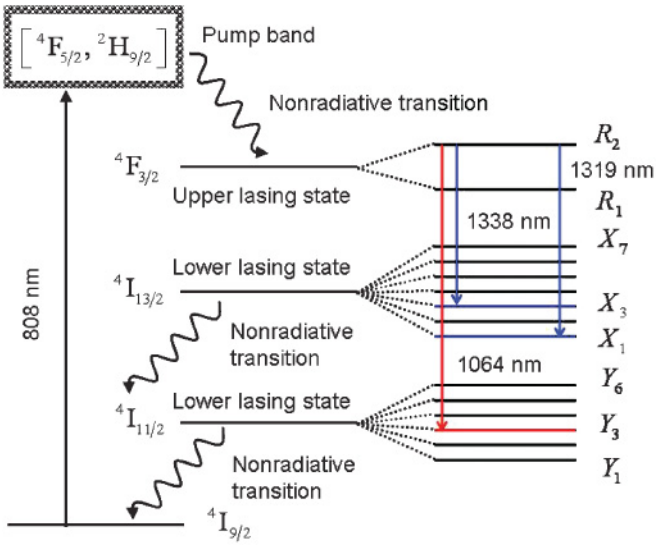

FIG. 8. (Color online) Partial energy level diagram of Nd:YAG. Pump power is provided by a diode laser with wavelength 808 nm. The Λ-type laser system is composed of levels X_1, X_3, and R_2.

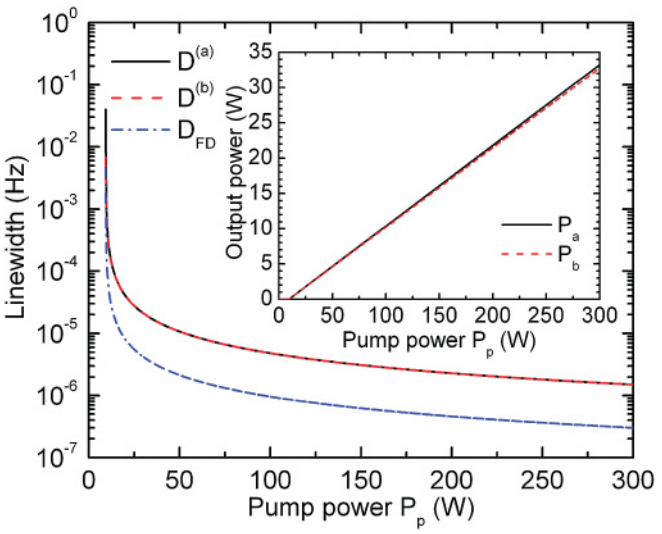

FIG. 9. (Color online) Dependence of linewidths and output powers (inset) of a Nd:YAG laser on the pump power P_p. The coherence between two laser fields well exceeds either laser field. P_a and P_b are the laser output powers corresponding to $|c\rangle$-$|a\rangle$ and $|c\rangle$-$|b\rangle$ laser transitions, respectively.

is a challenge to realize efficient cw multiwavelength operation at 1064 and 1319 nm [34] because of the large (∼5) ratio of the stimulated emission cross sections between $^4F_{3/2}$-$^4I_{11/2}$ ($\sigma_e = 45.8 \times 10^{-20}$ cm^2) and $^4F_{3/2}$-$^4I_{13/2}$ ($\sigma_e = 8.7 \times 10^{-20}$ cm^2) transitions [35].

Here we choose the Λ-type laser system being composed of $|a\rangle = X_1$, $|b\rangle = X_3$, and $|c\rangle = R_2$ with the laser wavelengths 1319 nm ($|c\rangle$-$|a\rangle$) and 1338 nm ($|c\rangle$-$|b\rangle$) as shown in Fig. 8. Theses two laser transitions have the close effective stimulated emission cross sections $\sigma_e(|c\rangle\text{-}|a\rangle) = 8.7 \times 10^{-20}$cm^2 and $\sigma_e(|c\rangle\text{-}|b\rangle) = 9.2 \times 10^{-20}$cm^2 [35], which make the dual-laser operation relatively easier. These two laser transitions have the branching ratios of $\beta(|c\rangle\text{-}|a\rangle) = 0.018$ and $\beta(|c\rangle\text{-}|b\rangle) = 0.021$, respectively, and the same full width at half maximum of the emission line $\Delta\nu(|c\rangle\text{-}|a\rangle) = \Delta\nu(|c\rangle\text{-}|b\rangle) = 4.5$ cm^{-1} [35].

The pump energy can be provided by a diode laser with wavelength 808 nm. Here we consider the longitudinal pumping case. We assume the pump beam is Gaussian with a waist $w_0 = 2$ mm. The length of the Nd:YAG crystal is $l = 10$ mm and the diameter of the cross section is $2w_0 = 4$ mm. Since the lifetime of $^4F_{3/2}$ is about $\tau(^4F_{3/2}) = 230$ μs, we have $\gamma_{ct} = 2\pi \times 692.0$ Hz, $\gamma_{ca} = 2\pi \times 12.5$ Hz, $\gamma_{cb} = 2\pi \times 14.5$ Hz, and $\gamma_c' = 2\pi \times 665.0$ Hz. In addition, the decay rates of two lower lasing $|a,b\rangle$ levels are about $\gamma_a = \gamma_b \simeq 120$ GHz [36]. We also have $\Gamma_A = (\gamma_{ct} + \gamma_a)/2$, $\Gamma_B = (\gamma_{ct} + \gamma_b)/2$, and $\Gamma_C = (\gamma_a + \gamma_b)/2$. The pump rate can be expressed as $R = f_{R_2}\eta_p \frac{P_p}{h\nu_p}$, where $\eta_p \sim 12.5\%$ [37] is the pump efficiency, P_p the pump power from the diode laser, h Planck's constant, and ν_p the angular frequency of the pump field.

From Fig. 2 we know that two laser fields oscillating can be realized only when two coupling strengths g_a and g_b are close to each other, and for $g_a = g_b$ one can get the maximum coherence between two laser fields. In this case, we need to choose cavity parameters to make g_a be equal to g_b. The atom-cavity coupling constants $g_{a,b}$ are given by $g_{a(b)} = \sqrt{\omega_{La(Lb)}/(2\hbar\epsilon_0 V_{a(b)})}|\mu_{a(b)}|$, where $|\mu_{a(b)}|$ is the magnitude of the transition matrix element corresponding to transition $|c\rangle$-$|a(b)\rangle$, and $V_{a(b)}$ is the volume of cavity coupling to the lasing transition $|c\rangle$-$|a(b)\rangle$. We need to use two cavities with different cavity-mode volumes to couple to the same atoms and get the same coupling constants $g_a = g_b$. For this reason, we choose the beam diameter of the cavity, which couples to the lasing transition $|c\rangle$-$|a\rangle$, to be $2w_a = 2w_0$ mm (w_a is the laser beam waist) and the beam diameter of the other cavity is $2w_b \simeq 2.2w_0$ mm. Both cavities have the same cavity length of about $L = 60$ cm. Therefore, all the atoms simultaneously contribute to two laser fields and two coupling constants are equal to each other $g_a = g_b = 2\pi \times 8.53$ Hz. The output ports of two cavities have the same amplitude reflectivity $r = 94.87\%$. Thus, we get the cavity loss rates $\kappa_a = \kappa_b = 2\pi \times 8.4$ MHz.

Figure 9 displays the dependence of linewidths and output powers of a Nd:YAG laser on the pump power P_p. Since the stimulated emission cross sections of two laser transitions are very close, the linewidths of two laser fields (1319 and 1338 nm) approach each other, and the coherence between the two lasers well exceeds that of either laser field because of the phase-matching effect. The laser output powers P_a ($|c\rangle$-$|a\rangle$) and P_b ($|c\rangle$-$|b\rangle$) coincide with the experimental result in Ref. [37]. Since two laser fields simultaneously oscillate inside a traveling-wave (not standing wave) cavity, each output power is nearly equal to that of the single field oscillating case. Additionally, the higher laser powers lead to a higher coherence between two laser fields.

VI. SPECTRUM OF THE OUTPUT FIELD

So far, we have discussed the laser fields inside the cavity. Moreover, one is interested in the output fields. The

relation between fields inside and outside the cavity has been established in Refs. [38–41]. Now we investigate the spectrum of fluctuations for the fields transmitted through the cavity port. From Ref. [1], the spectrum of the output fields can be expressed as

$$V_A(\omega) = 1 + 4\kappa_a\left(\delta X_A^2\right)_\omega, \tag{115}$$

$$V_B(\omega) = 1 + 4\kappa_b\left(\delta X_B^2\right)_\omega, \tag{116}$$

where $(\delta X_A^2)_\omega$ and $(\delta X_B^2)_\omega$ are the spectra of the amplitude quadrature components and can be derived from the autocorrelation functions of the amplitude quadratures,

$$\langle \delta X_A(\omega)\delta X_A(\omega')\rangle = \left(\delta X_A^2\right)_\omega \delta(\omega+\omega'), \tag{117}$$

$$\langle \delta X_B(\omega)\delta X_B(\omega')\rangle = \left(\delta X_B^2\right)_\omega \delta(\omega+\omega'), \tag{118}$$

where the amplitude quadratures are defined as

$$\delta X_A(\omega) = \tfrac{1}{2}[\delta\mathcal{A}(\omega) + \delta\mathcal{A}^*(\omega)], \tag{119}$$

$$\delta X_B(\omega) = \tfrac{1}{2}[\delta\mathcal{B}(\omega) + \delta\mathcal{B}^*(\omega)], \tag{120}$$

The constant 1 in Eq. (117) corresponds to the shot-noise contribution. For a coherent state, we have $V_{A,B} = 1$. Therefore, $V_{A,B} < 1$ means squeezing in a quadrature component, and $V_{A,B}(\omega) = 0$ denotes the complete squeezing at some frequency ω [42]. Actually, this spectrum defined in this way corresponds to the normalized photocurrent obtained in a homodyne measurement of the field quadrature component. Since the expressions of $V_{A,B}(\omega)$ are very complicated, we do not list them here and only show the consequences.

Figure 10 displays the spectra of amplitude fluctuations for two cases: ($\mathcal{A}_0 \neq 0$ and $\mathcal{B}_0 = 0$) and ($\mathcal{A}_0 \neq 0$ and $\mathcal{B}_0 \neq 0$) for a certain pumping rate. For simplicity, we only consider the laser oscillation with maximum coherence between two fields, e.g., the minimum $D_{\rm FD}$. In both cases, amplitude noise at low frequencies is reduced with increasing parameter p, and for a regular statistics $p = 1$ we obtain the limited noise reduction. However, the optical oscillation of field $\mathcal{B}_0$ can enlarge the amplitude noise for a certain parameter p because part of the pumping rate contributes to field $\mathcal{B}_0$ and the photon number $\mathcal{I}_{a0}$ is reduced as shown in Fig. 6(a), which makes the amplitude noises unable to be squeezed below the shot-noise level.

If we increase the coupling strength g_b from zero, the amplitude noise of field $\mathcal{A}_0$ is sharply enlarged when field $\mathcal{B}_0$ starts to oscillate. This is because field $\mathcal{B}_0$ has a large amplitude noise, which can be delivered to field $\mathcal{A}_0$ since they have the same upper lasing level. Then, the field amplitude noises of both fields decrease with two field intensities approaching each other and simultaneously arrive at the minimum amplitude noise when $\mathcal{I}_{a0} = \mathcal{I}_{b0}$.

VII. CONCLUSION

Up to now, great theoretical and practical interest has been focused on reducing quantum noise in lasers, such as the regularization of pumping [27], the correlated spontaneous emission lasers [7,8], and the reduction of spontaneous-emission noise for short measurement times due to the atomic memory effects [30].

Here we investigate the quantum-limited phase-matching effect in a Λ-type laser system, which is a universal physical model. For simplicity, we have considered the active medium to be homogeneously broadened. Unlike the similar physical model in Ref. [17], two quasimonochromatic fields are directly generated by two lasing transitions and the coherence between two laser fields is not limited by the saturation broadening. Our result shows that although either laser field has a high phase fluctuation, two field phases match each other and the final coherence between two fields can well exceed the linewidth of either laser. However, compared with the case of single field oscillating, the amplitude fluctuations of the output fields are enlarged and field squeezing is damaged. Additionally, based on a linear stability analysis of the steady-state solution, we find that the stability of the field steady state can substantially restrict the occurrence of this phase-matching effect in the bad-cavity limit for a high pump rate.

ACKNOWLEDGMENTS

This work was supported by the JSPS (ID No. P09229) and the National Natural Science Foundation of China (Grant No. 10874009).

APPENDIX: DIFFUSION COEFFICIENTS

1. Diffusion coefficients of the single-atom noise operators

Here we list the nonvanishing diffusion coefficients of the single-atom noise operators calculated from Eq. (13):

$$\mathfrak{d}(\sigma_A^+,\sigma_{aa}) = \gamma_a\langle\sigma_A^+(t)\rangle,$$
$$\mathfrak{d}(\sigma_A^+,\sigma_C) = (\Gamma_A + \Gamma_C - \Gamma_B)\langle\sigma_B^+(t)\rangle,$$
$$\mathfrak{d}(\sigma_A^+,\sigma_A) = [2\Gamma_A - (\gamma_c' + \gamma_{ca} + \gamma_{cb})]\langle\sigma_{cc}(t)\rangle,$$
$$\mathfrak{d}(\sigma_B^+,\sigma_C^+) = (\Gamma_B + \Gamma_C - \Gamma_A)\langle\sigma_A^+(t)\rangle,$$
$$\mathfrak{d}(\sigma_B^+,\sigma_B) = [2\Gamma_B - (\gamma_c' + \gamma_{ca} + \gamma_{cb})]\langle\sigma_{cc}(t)\rangle,$$
$$\mathfrak{d}(\sigma_B^+,\sigma_{bb}) = \gamma_b\langle\sigma_B^+(t)\rangle,$$
$$\mathfrak{d}(\sigma_C^+,\sigma_{aa}) = \gamma_a\langle\sigma_C^+(t)\rangle,$$
$$\mathfrak{d}(\sigma_C^+,\sigma_C) = \gamma_{cb}\langle\sigma_{cc}(t)\rangle + (2\Gamma_C - \gamma_b)\langle\sigma_{bb}(t)\rangle,$$

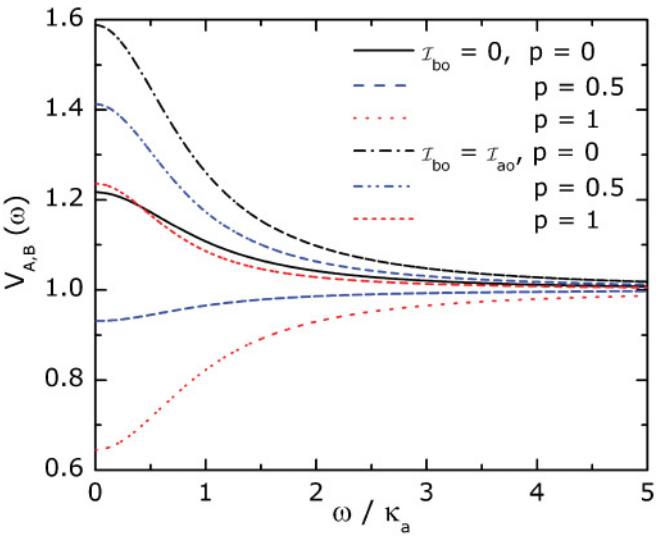

FIG. 10. (Color online) Spectraof amplitude fluctuations with pumping rate $R/R_{\rm TH}^{(a,0)} = 10^3$ and $g_b = g_a$. All the other parameters are the same as in Fig. 4.

$$\mathfrak{d}(\sigma_{aa},\sigma_{aa}) = \gamma_a\langle\sigma_{aa}(t)\rangle + \gamma_{ca}\langle\sigma_{cc}(t)\rangle,$$
$$\mathfrak{d}(\sigma_{aa},\sigma_{cc}) = -\gamma_{ca}\langle\sigma_{cc}(t)\rangle,$$
$$\mathfrak{d}(\sigma_{bb},\sigma_{cc}) = -\gamma_{cb}\langle\sigma_{cc}(t)\rangle,$$
$$\mathfrak{d}(\sigma_{bb},\sigma_{bb}) = \gamma_b\langle\sigma_{bb}(t)\rangle + \gamma_{cb}\langle\sigma_{cc}(t)\rangle,$$
$$\mathfrak{d}(\sigma_{cc},\sigma_{cc}) = (\gamma_c' + \gamma_{ca} + \gamma_{cb})\langle\sigma_{cc}(t)\rangle.$$

All the other diffusion coefficients are zero.

2. Diffusion coefficients of the macroscopic atomic noise operators

Using the definitions of macroscopic Langevin forces defined by Eqs. (32)–(37), one can derive the following nonvanishing diffusion coefficients:

$$\mathfrak{D}(M_A^+,N_{aa}) = \gamma_a\langle M_A^+(t)\rangle,$$
$$\mathfrak{D}(M_A^+,M_A) = R + [2\Gamma_A - (\gamma_c' + \gamma_{ca} + \gamma_{cb})]\langle N_{cc}(t)\rangle,$$
$$\mathfrak{D}(M_A^+,M_C) = (\Gamma_A + \Gamma_C - \Gamma_B)\langle M_B^+(t)\rangle,$$
$$\mathfrak{D}(M_B^+,M_C^+) = (\Gamma_B + \Gamma_C - \Gamma_A)\langle M_A^+(t)\rangle,$$
$$\mathfrak{D}(M_B^+,N_{bb}) = \gamma_b\langle M_B^+(t)\rangle,$$
$$\mathfrak{D}(M_B^+,M_B) = R + [2\Gamma_B - (\gamma_c' + \gamma_{ca} + \gamma_{cb})]\langle N_{cc}(t)\rangle,$$
$$\mathfrak{D}(M_C^+,N_{aa}) = \gamma_a\langle M_C^+(t)\rangle,$$
$$\mathfrak{D}(M_C^+,M_C) = \gamma_{cb}\langle N_{cc}(t)\rangle + (2\Gamma_C - \gamma_b)\langle N_{bb}(t)\rangle,$$
$$\mathfrak{D}(N_{aa},N_{aa}) = \gamma_a\langle N_{aa}(t)\rangle + \gamma_{ca}\langle N_{cc}(t)\rangle,$$
$$\mathfrak{D}(N_{aa},N_{cc}) = -\gamma_{ca}\langle N_{cc}(t)\rangle,$$
$$\mathfrak{D}(N_{bb},N_{cc}) = -\gamma_{cb}\langle N_{cc}(t)\rangle,$$
$$\mathfrak{D}(N_{bb},N_{bb}) = \gamma_b\langle N_{bb}(t)\rangle + \gamma_{cb}\langle N_{cc}(t)\rangle,$$
$$\mathfrak{D}(N_{cc},N_{cc}) = R(1-p) + (\gamma_c' + \gamma_{ca} + \gamma_{cb})\langle N_{cc}(t)\rangle.$$

In our derivations, we used

$$\left\langle \sum_{j\neq k} \delta(t-t_j)\delta(t'-t_k) \right\rangle_S = R^2 - pR\delta(t-t'), \quad \text{(A1)}$$

where p is a parameter which characterizes the pumping statistics: Poissonian excitation statistics correspond to $p = 0$, and for regular statistics we have $p = 1$. The intermediate cases between these two extremes are described by values of p between 0 and 1.

3. Diffusion coefficients of the *c*-number macroscopic atomic noise variables

Following Eq. (50), one can find all the nonvanishing c-number diffusion coefficients as follows:

$$\mathcal{D}(\mathcal{M}_A^*,\mathcal{M}_A^*) = 2g_a\langle\mathcal{A}^*(t)\mathcal{M}_A^*(t)\rangle,$$
$$\mathcal{D}(\mathcal{M}_A^*,\mathcal{M}_B^*) = g_a\langle\mathcal{A}^*(t)\mathcal{M}_B^*(t)\rangle + g_b\langle\mathcal{B}^*(t)\mathcal{M}_A^*(t)\rangle,$$
$$\mathcal{D}(\mathcal{M}_A^*,\mathcal{M}_C^*) = g_a\langle\mathcal{A}^*(t)\mathcal{M}_C^*(t)\rangle,$$
$$\mathcal{D}(\mathcal{M}_A^*,\mathcal{N}_{aa}) = \gamma_a\langle\mathcal{M}_A^*(t)\rangle,$$
$$\mathcal{D}(\mathcal{M}_B^*,\mathcal{M}_B^*) = 2g_b\langle\mathcal{B}^*(t)\mathcal{M}_B^*(t)\rangle,$$
$$\mathcal{D}(\mathcal{M}_B^*,\mathcal{M}_C^*) = (\Gamma_B + \Gamma_C - \Gamma_A)\langle\mathcal{M}_A^*(t)\rangle + g_a\langle\mathcal{A}^*(t)[\mathcal{N}_{bb}(t) - \mathcal{N}_{aa}(t)]\rangle - g_b\langle\mathcal{B}^*(t)\mathcal{M}_C^*(t)\rangle,$$
$$\mathcal{D}(\mathcal{M}_B^*,\mathcal{N}_{aa}) = g_a\langle\mathcal{A}^*(t)\mathcal{M}_C(t)\rangle,$$
$$\mathcal{D}(\mathcal{M}_B^*,\mathcal{N}_{bb}) = \gamma_b\langle\mathcal{M}_B^*(t)\rangle - g_a\langle\mathcal{A}^*(t)\mathcal{M}_C(t)\rangle,$$
$$\mathcal{D}(\mathcal{M}_C^*,\mathcal{N}_{aa}) = \gamma_a\langle\mathcal{M}_C^*(t)\rangle,$$
$$\mathcal{D}(\mathcal{M}_C^*,\mathcal{N}_{bb}) = -g_a\langle\mathcal{A}^*(t)\mathcal{M}_B(t)\rangle - g_b\langle\mathcal{M}_A^*(t)\mathcal{B}(t)\rangle,$$
$$\mathcal{D}(\mathcal{M}_C^*,\mathcal{N}_{cc}) = g_a\langle\mathcal{A}^*(t)\mathcal{M}_B(t)\rangle + g_b\langle\mathcal{M}_A^*(t)\mathcal{B}(t)\rangle,$$
$$\mathcal{D}(\mathcal{M}_C^*,\mathcal{M}_A) = (\Gamma_A + \Gamma_C - \Gamma_B)\langle\mathcal{M}_B(t)\rangle,$$
$$\mathcal{D}(\mathcal{M}_A^*,\mathcal{M}_A) = [2\Gamma_A - (\gamma_c' + \gamma_{cb} + \gamma_{ca})]\langle\mathcal{N}_{cc}(t)\rangle + R,$$
$$\mathcal{D}(\mathcal{M}_B^*,\mathcal{M}_B) = [2\Gamma_B - (\gamma_c' + \gamma_{cb} + \gamma_{ca})]\langle\mathcal{N}_{cc}(t)\rangle + R,$$
$$\mathcal{D}(\mathcal{M}_C^*,\mathcal{M}_C) = \gamma_{cb}\langle\mathcal{N}_{cc}(t)\rangle + (2\Gamma_C - \gamma_b)\langle\mathcal{N}_{bb}(t)\rangle - g_a[\langle\mathcal{M}_A^*(t)\mathcal{A}(t)\rangle + \langle\mathcal{A}^*(t)\mathcal{M}_A(t)\rangle],$$
$$\mathcal{D}(\mathcal{N}_{aa},\mathcal{N}_{aa}) = \gamma_a\langle\mathcal{N}_{aa}(t)\rangle + \gamma_{ca}\langle\mathcal{N}_{cc}(t)\rangle - g_a\langle\mathcal{M}_A^*(t)\mathcal{A}(t)\rangle - g_a\langle\mathcal{A}^*(t)\mathcal{M}_A(t)\rangle,$$
$$\mathcal{D}(\mathcal{N}_{aa},\mathcal{N}_{cc}) = -\gamma_{ca}\langle\mathcal{N}_{cc}(t)\rangle + g_a\langle\mathcal{M}_A^*(t)\mathcal{A}(t)\rangle + g_a\langle\mathcal{A}^*(t)\mathcal{M}_A(t)\rangle,$$
$$\mathcal{D}(\mathcal{N}_{bb},\mathcal{N}_{bb}) = \gamma_b\langle\mathcal{N}_{bb}(t)\rangle + \gamma_{cb}\langle\mathcal{N}_{cc}(t)\rangle - g_b\langle\mathcal{M}_B^*(t)\mathcal{B}(t)\rangle - g_b\langle\mathcal{B}^*(t)\mathcal{M}_B(t)\rangle,$$
$$\mathcal{D}(\mathcal{N}_{bb},\mathcal{N}_{cc}) = -\gamma_{cb}\langle\mathcal{N}_{cc}(t)\rangle + g_b\langle\mathcal{M}_B^*(t)\mathcal{B}(t)\rangle + g_b\langle\mathcal{B}^*(t)\mathcal{M}_B(t)\rangle,$$
$$\mathcal{D}(\mathcal{N}_{cc},\mathcal{N}_{cc}) = R(1-p) + (\gamma_c' + \gamma_{cb} + \gamma_{ca})\langle\mathcal{N}_{cc}(t)\rangle - g_a\langle\mathcal{M}_A^*(t)\mathcal{A}(t)\rangle - g_a\langle\mathcal{A}^*(t)\mathcal{M}_A(t)\rangle - g_b\langle\mathcal{M}_B^*(t)\mathcal{B}(t)\rangle - g_b\langle\mathcal{B}^*(t)\mathcal{M}_B(t)\rangle.$$

[1] M. I. Kolobov, L. Davidovich, E. Giacobino, and C. Fabre, Phys. Rev. A **47**, 1431 (1993).
[2] H. Haken, *Laser Theory* (Springer-Verlag, Berlin, 1984).
[3] M. Lax, in *Physics of Quantum Electronics*, edited by P. L. Kelley, B. Lax, and P. E. Tannenwald (McGraw-Hill, New York, 1966).
[4] A. L. Schawlow and C. H. Townes, Phys. Rev. **112**, 1940 (1958).
[5] S. J. M. Kuppens, M. P. van Exter, and J. P. Woerdman, Phys. Rev. Lett. **72**, 3815 (1994).
[6] Deshui Yu and Jingbiao Chen, Phys. Rev. A **78**, 013846 (2008).
[7] M. O. Scully, Phys. Rev. Lett. **55**, 2802 (1985).
[8] M. O. Scully and M. S. Zubairy, Phys. Rev. A **35**, 752 (1987).
[9] Deshui Yu and Jingbiao Chen, Phys. Rev. A **81**, 023818 (2010).
[10] F. Haake, M. I. Kolobov, C. Fabre, E. Giacobino, and S. Reynaud, Phys. Rev. Lett. **71**, 995 (1993).
[11] F. Haake, M. I. Kolobov, C. Seeger, C. Fabre, E. Giacobino, and S. Reynaud, Phys. Rev. A **54**, 1625 (1996).
[12] C. Seeger, M. I. Kolobov, M. Kus, and F. Haake, Phys. Rev. A **54**, 4440 (1996).
[13] Deshui Yu and Jingbiao Chen, Phys. Rev. A **81**, 053809 (2010).
[14] M. Fleischhauer, Phys. Rev. Lett. **72**, 989 (1994).
[15] M. Fleischhauer and T. Richter, Phys. Rev. A **51**, 2430 (1995).
[16] E. E. Mikhailov, V. A. Sautenkov, Y. V. Rostovtsev, A. Zhang, M. S. Zubairy, M. O. Scully, and G. R. Welch, Phys. Rev. A **74**, 013807 (2006).
[17] Deshui Yu and Jingbiao Chen, Phys. Rev. Lett. **98**, 050801 (2007).
[18] Long-Sheng Ma, Zhiyi Bi, A. Bartels, L. Robertsson, M. Zucco, R. S. Windeler, G. Wilpers, C. Oates, L. Hollberg, and S. A. Diddams, Science **303**, 1843 (2004).
[19] V. J. Sanchez-Morcillo, E. Roldan, and G. J. de Valcarel, Quantum Semiclass. Opt. **7**, 889 (1995).
[20] A. G. Vladimirov, P. Mandel, S. F. Yelin, M. D. Lukin, and M. O. Scully, Phys. Rev. E **57**, 1499 (1998).
[21] O. Kocharovskaya, R. Kolesov, and Y. Rostovtsev, Laser Physics **9**, 745 (1999).
[22] A. Nottelmann, C. Peters, and W. Lange, Phys. Rev. Lett. **70**, 1783 (1993).
[23] K. Zaheer, Phys. Rev. A **49**, 2914 (1994).
[24] M. Sargent III, M. O. Scully, and W. E. Lamb Jr., *Laser Physics* (Addison-Wesley, Reading, MA, 1974).
[25] M. O. Scully and M. S. Zubairy, *Quantum Optics* (Cambridge University, Cambridge, England, 1997).
[26] M. Orszag, *Quantum Optics: Including Noise Reduction, Trapped Ions, Quantum Trajectories, and Decoherence* (Springer-Verlag, Berlin, 2000).
[27] C. Benkert, M. O. Scully, J. Bergou, L. Davidovich, M. Hillery, and M. Orszag, Phys. Rev. A **41**, 2756 (1990).
[28] G. H. M. van Tartwijk and G. P. Agrawal, Prog. Quantum Electron. **22**, 43 (1998).
[29] Ya. I. Khanin, *Fundamentals of Laser Dynamics* (Cambridge International Science Publishing, New York, 2005).
[30] C. Benkert, M. O. Scully, and G. Sussmann, Phys. Rev. A **41**, 6119 (1990).
[31] C. Benkert, M. O. Scully, A. A. Rangwala, and W. Schleich, Phys. Rev. A **42**, 1503 (1990).
[32] L. Davidovich, Rev. Mod. Phys. **68**, 127 (1996).
[33] E. V. Zharikov, N. N. Il'ichev, V. V. Laptev, A. A. Malyutin, V. G. Ostroumov, P. P. Pashinin, and I. A. Shcherbakov, Sov. J. Quantum Electron. **12**, 338 (1982).
[34] Baole Lu, Haowei Chen, Jiaxi Guo, Man Jiang, Renjian Zhang, Jintao Bai, and Zhaoyu Ren, Opt. Commun. **284**, 1941 (2011).
[35] S. Singh, R. G. Smith, and L. G. Van Uitert, Phys. Rev. B **10**, 2566 (1974).
[36] O. Svelto, *Principles of Lasers* (Springer, New York, 1998).
[37] Junhua Lu, J. Lu, T. Murai, K. Takaichi, T. Uematsu, Jianqiu Xu, K. Ueda, H. Yagi, T. Yanagitani, and A. A. Kaminskii, Opt. Lett. **27**, 1120 (2002).
[38] M. J. Collett and C. W. Gardiner, Phys. Rev. A **30**, 1386 (1984).
[39] C. M. Caves and B. L. Schumaker, Phys. Rev. A **31**, 3068 (1985).
[40] C. W. Gardiner and M. J. Collett, Phys. Rev. A **31**, 3761 (1985).
[41] B. L. Schumaker and C. M. Caves, Phys. Rev. A **31**, 3093 (1985).
[42] M. T. Fontenelle and L. Davidovich, Phys. Rev. A **51**, 2560 (1995).